Lebanese American University Repository (LAUR)

Post-print version/Author Accepted Manuscript

Publication metadata:

Title: Breathing regulation and blood gas homeostasis after near complete lesions of the retrotrapezoid nucleus in adult rats

Author(s): Souza, George M.P.; Kanbar, Roy; Stornetta, Daniel S.; Abbott, Stephen B.G.; Stornetta, Ruth L.; Guyenet, Patrice G.

Journal: The Journal of physiology

DOI/Link: https://doi.org/10.1113/JP275866

How to cite this post-print from LAUR:

Souza, G. M., Kanbar, R., Stornetta, D. S., Abbott, S. B., Stornetta, R. L., & Guyenet, P. G. (2018). Breathing regulation and blood gas homeostasis after near complete lesions of the retrotrapezoid nucleus in adult rats, DOI: https://doi.org/10.1113/JP275866 /Handle: http://hdl.handle.net/10725/11476

C 2018

This Open Access post-print is licensed under a Creative Commons Attribution-Non Commercial-No Derivatives (CC-BY-NC-ND 4.0)

This paper is posted at LAU Repository
For more information, please contact: archives@lau.edu.lb

Accepted Article

DOI: 10.1113/JP275866

Breathing regulation and blood gas homeostasis after near complete lesions of the retrotrapezoid nucleus in adult rats

George M.P.R. Souza[1*], Roy Kanbar[2*], Daniel S. Stornetta[1], Stephen B.G. Abbott[1], Ruth L. Stornetta[1] and Patrice G. Guyenet[1]

[1] *Department of Pharmacology, University of Virginia, Charlottesville, VA 22908*
[2] *Department of Pharmaceutical Sciences, Lebanese American University, Beyrouth, Lebanon*
** co-first authors*

Abbreviated title: RTN, breathing and PCO_2 homeostasis

George Souza received a PhD in Physiology from the University of Sao Paulo, Brazil (2017). Currently, he is a post-doctoral fellow in the University of Virginia (UVA). He has been and still working on central control of breathing and blood pressure with focus on the role of specific brainstem neurons involved in these functions.

Indexing terms: central respiratory chemoreceptors, carotid bodies, breathing, breathing and sleep

Address correspondence to:

Patrice G. Guyenet, PhD
University of Virginia Health System
P.O. Box 800735, 1300 Jefferson Park Avenue
Charlottesville, VA 22908-0735.
Tel: (434) 924-5849; Fax: (434) 982-3878; E-mail: pgg@virginia.edu

This is an Accepted Article that has been peer-reviewed and approved for publication in the The Journal of Physiology, but has yet to undergo copy-editing and proof correction. Please cite this article as an 'Accepted Article'; doi: 10.1113/JP275866.

This article is protected by copyright. All rights reserved.

Accepted Article

ABSTRACT

The retrotrapezoid nucleus (RTN) is one of several CNS nuclei that contribute, in various capacities (e.g. CO_2 detection, neuronal modulation) to the central respiratory chemoreflex (CRC). Here we test how important the RTN is to PCO_2 homeostasis and breathing during sleep or wake. RTN *Nmb* positive neurons were killed with targeted microinjections of substance-P-saporin conjugate in adult rats. Under normoxia, rats with large RTN lesions (92 ± 4 % cell loss) had normal blood pressure (BP) and arterial pH but were hypoxic (-8 mmHg PaO_2) and hypercapnic (+10 mmHg $PaCO_2$). In resting conditions, minute-volume (V_E) was normal but breathing frequency (f_R) was elevated and tidal volume (V_T) reduced. Resting O_2 consumption and CO_2 production were normal. The hypercapnic ventilatory reflex in 65% FiO_2 had an inverse exponential relationship with the number of surviving RTN neurons and was decreased by up to 92%. The hypoxic ventilatory reflex (HVR; FiO_2 21-10%) persisted after RTN lesions, hypoxia-induced sighing was normal and hypoxia-induced hypotension reduced. In rats with RTN lesions, breathing was lowest during slow-wave sleep (SWS), especially under hyperoxia, but apneas and sleep-disordered breathing were not observed.

In conclusion, near complete RTN destruction in rats virtually eliminates the CRC but HVR persists and sighing and the state-dependence of breathing are unchanged. Under normoxia, RTN lesions cause no change in V_E but alveolar ventilation is reduced by at least 21%, probably because of increased physiological dead volume. RTN lesions do not cause sleep apnea during SWS, even under hyperoxia.

This article is protected by copyright. All rights reserved.

Accepted Article

KEY POINTS SUMMARY

- Background: the retrotrapezoid nucleus (RTN) drives breathing proportionally to brain PCO_2 but its role during various states of vigilance needed clarification.
- New result: Under normoxia, RTN lesions increase the arterial PCO_2 set-point, lower the PO_2 set-point and reduce alveolar ventilation relative to CO_2 production. Tidal volume is reduced and breathing frequency increased to a comparable degree during wake, slow-wave sleep and REM sleep. RTN lesions do not produce apneas or disordered breathing during sleep.
- New result: RTN lesions in rats virtually eliminate the central respiratory chemoreflex (CRC) while preserving the cardiorespiratory responses to hypoxia; the relationship between CRC and number of surviving RTN *Nmb* neurons is an inverse exponential.
- Conclusions: the CRC does not function without the RTN. In the quasi-complete absence of the RTN and CRC, alveolar ventilation is reduced despite an increased drive to breathe from the carotid bodies.

INTRODUCTION

Arterial PCO_2 homeostasis requires continual breathing adjustments via feedback from the carotid bodies (peripheral chemoreceptors) and central chemoreceptors (Kumar & Prabhakar, 2012; Nattie, 2012). Many CNS nuclei contribute to the breathing stimulation elicited by a rise in CNS PCO_2 (central respiratory chemoreflex, CRC), including the retrotrapezoid nucleus (RTN) and subsets of serotonergic, catecholaminergic and orexinergic neurons (Gargaglioni *et al.*, 2010; Li & Nattie, 2010; Ray *et al.*, 2011; Nattie, 2012; Brust *et*

This article is protected by copyright. All rights reserved.

Accepted Article

al., 2014; Teran *et al.*, 2014; Guyenet *et al.*, 2017). The contribution of these neurons to the CRC is often behavior and state-dependent (e.g. orexin) and relies, in variable and unknown proportion, on their ability to directly respond to local changes in brain PCO_2 or to facilitate the ventilatory response elicited by CO_2-activated neurons.

RTN neurons appear to play a pivotal integrative role in the CRC. These glutamatergic neurons innervate selectively the brainstem respiratory centers, encode local brain PCO_2, drive the respiratory network in proportion to arterial blood acidity and are strongly activated by serotonin, noradrenaline and orexin. The importance of the RTN to the CRC is most strongly supported by the results of genetic manipulations in mice. For example, preventing RTN development or simultaneously knocking out two genes (*Kcnk5* and *Gpr4*) required for the pH-sensitivity of RTN neurons in brain slices virtually eliminates the hypercapnic ventilatory reflex (HCVR) (Gestreau *et al.*, 2010; Ramanantsoa *et al.*, 2011; Kumar *et al.*, 2015; Ruffault *et al.*, 2015; Guyenet *et al.*, 2016). This genetic evidence has certain limitations. Disrupting RTN formation during embryogenesis could have cascading effects on the development of other parts of the respiratory pattern generator. *Kcnk5* and *Gpr4* are prominently expressed by the kidneys, a key organ for acid-base control, and the CNS expression of *Kcnk5* and *Gpr4* is neither restricted to the RTN (*Kcnk5*) nor to neurons (*Gpr4*) (Mahadevan *et al.*, 1995; Reyes *et al.*, 1998; Gestreau *et al.*, 2010; Dong *et al.*, 2017). Finally, the HCVR of $Phox2b^{27alacki}$; $Egr\text{-}2^{cre}$ mice, in which the RTN fails to develop, recovers in adulthood to approximately 40% of control (Ramanantsoa *et al.*, 2011).

The importance of the RTN has also been tested by lesions of this nucleus with a saporin conjugate ([Sar^9,$Met(O_2)^{11}$]-substance P, SSP-SAP), that destroys substance P receptor- (*Tacr*-) expressing neurons (Nattie & Li, 2002a; Takakura *et al.*, 2008; 2014; Shi *et al.*, 2016; 2017). In adult unanesthetized rats, this procedure only causes a modest and

This article is protected by copyright. All rights reserved.

Accepted Article

transient reduction of the HCVR (Nattie & Li, 2002a; Takakura *et al.*, 2014), however this reflex is reduced by around 60% if the carotid bodies are simultaneously denervated (Takakura *et al.*, 2014). That 40% of the HCVR persists after RTN lesions in carotid body-denervated animals can be interpreted in several ways. First, the RTN may not be uniquely important to the CRC, as proposed by several investigators (Nattie, 2012; Teran *et al.*, 2014). Second, the survival of a very small fraction of RTN neurons may be sufficient to preserve a large portion of the CRC. Indeed, the difficulty to identify the key neurons and to gauge the extent of their destruction remains the main limitation of such lesion studies. In the case of the RTN, early studies were unable to quantify the degree of cell loss due to a lack of cell specific markers (Nattie & Li, 2002a), whereas more recent studies assessed cell loss using immunohistochemical staining for *Phox2b*, a validated but not completely selective marker of the CO_2-responsive neurons (Stornetta *et al.*, 2006; Shi *et al.*, 2017). And finally, combined elimination of the RTN and the carotid bodies produces severe and sustained hypoventilation (Takakura *et al.*, 2014) which presumably raises resting arterial and brain PCO_2 well beyond the physiological range; the residual 40% HCVR observed in these animals could result from wide-spread, potentially non-selective, excitatory effects of CNS acidosis.

In the present study we assessed the importance of the RTN to PCO_2 homeostasis and the ventilatory reflexes of unanesthetized adult rats using unrestrained whole-body plethysmography, while measuring arterial blood gases, EEG, and blood pressure. We used SSP-SAP to destroy NK1R-expressing neurons in the RTN. In contrast to previous studies, the lesion was quantified using *Nmb* mRNA, which is a more precise marker of RTN neurons in adult rodents (Li *et al.*, 2016; Shi *et al.*, 2017). We tested the integrity of the cardiovascular and respiratory components of the peripheral chemoreflex and evaluated the contribution of the carotid bodies to the HCVR using hyperoxia rather than denervation to avoid collateral damage to baroreceptors, as well as the effects of severe chronic hypoventilation and network

This article is protected by copyright. All rights reserved.

remodeling. Finally, we examined the rats during both sleep and wake to find out whether RTN lesions cause sleep-disordered breathing.

Accepted Article

MATERIALS AND METHODS

Ethical Approval

We used 44 adult male Sprague-Dawley rats (300-400g; Taconic, Germantown, NY, USA). All the experimental procedures were in accordance with National Institutes of Health's *Guide for Care and Use of Laboratory Animals* and were approved by the University of Virginia Animal Care and Use Committee. The study complied with the ethical principles of *The Journal of Physiology*, and the experiments complied with the journal's animals ethics principles and regulation checklist (Grundy, 2015). Animals were housed under a standard artificial 12h light/dark cycle with water and food provided *ad libitum*.

Toxin injection and electrode implantation

To kill RTN neurons we injected a conjugate of saporin ([Sar^9,$Met(O_2)^{11}$]-substance P (SP-SAP; Advanced Targeting Systems, San Diego, CA, USA) which preferentially destroys neurons that express substance P receptors (Wiley & Lappi, 1999; Nattie & Li, 2002a; Takakura *et al.*, 2008). Injections were made bilaterally under electrophysiological guidance as described previously (Takakura *et al.*, 2008). Briefly, rats were anesthetized with a mixture of ketamine (75 $mg \cdot kg^{-1}$) and xylazine (5 $mg \cdot kg^{-1}$) and acepromazine (1 $mg \cdot kg^{-1}$) administered i.m. The adequacy of the anesthesia was judged by the lack of reflex in response to a firm tail pinch. Additional anesthetic was administered during the surgery if necessary (25% of the original dose, i.m.). All surgical procedures were conducted under aseptic

This article is protected by copyright. All rights reserved.

Accepted Article

conditions. Body temperature was kept close to 37°C with a servo-controlled heating pad. A small incision was made in both cheeks to reveal the mandibular branch of the facial nerve. The rat was placed in a stereotaxic apparatus (David Kopf Instruments, San Diego, CA, USA), with the bite bar set at 3.5 mm below the interaural line for a flat skull. SSP-SAP was loaded into glass micropipettes (25 µm tip, external diameter) and the location of the electrode tip relative to the facial motor nucleus was identified by recording antidromic field potentials elicited by facial nerve stimulation (Takakura *et al.*, 2008). A total of 6 microinjections (120 nl/injection; 3 rostrocaudally aligned injections per side) were made 100-200 µm below the lower edge of the facial motor nucleus 2 mm lateral to the midline. Experimental rats received either 0.6 ng, 1.2 ng, or 2.4 ng of SSP-SAP per injection. Control rats received injections of pH 7.35 phosphate buffered saline rather than unconjugated saporin because the exact mechanism by which RTN neurons were damaged was immaterial but we wished the surgical controls to have as little RTN damage as possible. The microinjections were immediately followed by electrode implantation. For EEG recording, 3 stainless screws were inserted extradurally as described previously (Basting *et al.*, 2015). Two additional wires were implanted in the superficial dorsal neck muscle to record the EMG. The wires were connected to pins (A-M System, Sequim, WA, USA) that were inserted in a plastic headstage (A-M System, Sequim, WA, USA). The headstage was fixed to the skull using a two part epoxy (Loctite, Westlake, OH, USA). After the surgery, an antibiotic (Ampicillin, 125 $mg \cdot kg^{-1}$, i.p.) and an analgesic (Ketoprofen, 3-5 $mg \cdot kg^{-1}$, subcutaneously) was administered. These drugs were re-administered 24 hrs later and the rats were monitored daily for the next three days. The animals were left to recover for at least 3 weeks before the next stage of the experiment.

This article is protected by copyright. All rights reserved.

Accepted Article

Blood pressure and arterial blood gases measurements

Rats were anesthetized with isoflurane (2.5% via nose cone). Isoflurane was administered in room air because rats with RTN lesions stopped breathing if given this anesthetic in pure oxygen. A polyethylene catheter (P-10 connected to P-50, Clay Adams, Parssipany, NJ, USA) was introduced into a femoral artery through a small skin incision and pushed towards the abdominal aorta. The arterial catheter was then tunneled under the skin and the tip was exteriorized in the dorsal aspect of the neck. Following surgery, the analgesic ketoprofen (3-5 $mg \cdot kg^{-1}$, s.c.) and the antibiotic ampicillin (125 $mg \cdot kg^{-1}$, i.p.) were administered. Rats were allowed to recover overnight. BP recording and blood gas sampling were done the next day. Arterial blood gases, plasma bicarbonate and arterial pH were measured using a handheld iStat configured with CG8+ cartridges (Abbott Instruments, Lake Bluff, Illinois, USA). For BP recording, the arterial catheter was connected to a pressure transducer. Following amplification, the signal was digitized at 1 kHz.

Physiological experiments in freely behaving rats

Physiological experiments were conducted three to four weeks after bilateral injection of SSP-SAP or saline in two stages. The effects of sleep and hyperoxia on breathing (Figs. 9, 10 except panel D, 11 and 12) were studied before arterial catheter implantation to avoid the disruptive effect of postsurgical stress. The rest of the experiments (cardiorespiratory reflexes, blood gases) were performed after catheter implantation. The rats were placed in a plethysmographic chamber (5L, EMKA Technologies, Falls Church, VA, USA) on two consecutive days prior to the experiment to habituate them to these surroundings. On the day of the recordings, rats were briefly anesthetized with isoflurane (2.0 % in room air) to connect the head-set EEG/EMG electrodes to the amplifier and, if the experiment required it, the arterial catheter was connected to the pressure transducer. The rats were then placed in the

This article is protected by copyright. All rights reserved.

Accepted Article

plethysmographic chamber. Recordings were initiated at least one hour later, when the animals were quietly awake or sleeping. The plethysmography chamber was continuously perfused with room air or, as required by the protocols, with various mixtures of O_2, N_2 and CO_2 (total flow: 1.5 $l \cdot min^{-1}$). The gas mixtures were produced by flow-mass controllers operated by FlowVision software (Alicat Scientific, Inc., Tucson, AZ, USA). The ventilatory reflex was measured by exposing the rats to 3, 6, and 9% $FiCO_2$ on a background of hyperoxia (65% FiO_2) to reduce the contribution of the carotid bodies to the hypercapnic stimulus (protocol shown in Fig. 4A). Blood gases were measured three times: under normoxia, 2-3 minutes after administration of hyperoxia and a third time while the rats were exposed to 9% $FiCO_2$ (Fig. 4A, arrowheads). Respiratory frequency (f_R), tidal volume (V_T) and minute-volume (V_E) were measured at the time indicated by the arrows in Fig. 4A. Rats were either quietly resting and/or in slow-wave sleep when the data were acquired. Periods of REM sleep were excluded from the analysis because f_R and V_T are highly variable and the chemoreflexes drastically reduced during this sleep stage (Coote, 1982; Burke *et al.*, 2015a).

Oxygen consumption (VO_2) and CO_2 production (VCO_2) were measured in metabolic chambers coupled with gas sensors (Oxymax Economy System, Columbus Instruments, OH, USA). Metabolic chambers were flushed with constant room air at 2 $l \cdot min^{-1}$. After one hour of acclimatization to the chambers, measurements were made automatically during three hours. Gas samples were analyzed every 10 minutes and average values of VO_2 and VCO_2 were expressed in $ml \cdot min \cdot 100g^{-1}$.

Data acquisition and analysis of physiological variables

Data were acquired using Spike2 software (version 7.03, Cambridge Electronics Design, Cambridge, UK) as described previously. Briefly, raw plethysmography signals were

This article is protected by copyright. All rights reserved.

Accepted Article

produced by a differential pressure transducer connected to the chamber, amplified (x500, EMKA technologies, Falls Church, VA, USA) and digitized at 1 kHz. Respiratory frequency (f_R, in breath·min^{-1}) and tidal volume, V_T, were derived from the flow signal using Spike2, 7.03. Tidal volume (V_T, area under the curve of the inspiratory flow), was calibrated against the signal generated by injecting 5 ml of dry air into the chamber with a syringe and expressed as ml per 100g body weight. Minute-volume (V_E), the product of f_R x V_T, was expressed in ml·min·100g^{-1}. Breathing variability was determined using the coefficient of variance (standard deviation divided by the mean of the breath-to-breath interval of 30 consecutive breaths). EEG and EMG signals were amplified (x1000, Harvard Apparatus, Holliston, MA, USA), bandpass filtered (EEG: 0.1-100 Hz, EMG: 100-3000 Hz) and digitized at 1 kHz. The state of vigilance of the rats was identified using conventional criteria. Non-REM sleep (slow wave sleep, SWS) was identified by the animal's posture, the predominance of high amplitude delta oscillations in the EEG (0.5-4 Hz), the low level of neck EMG activity and a very regular breathing pattern. The quiet awake state was identified by reduced power and desynchronized EEG, tonic neck EMG and a regular breathing rate. REM sleep was characterized by stable theta oscillations on the EEG (6-8 Hz), neck muscle atonia and a highly variable breathing with increased average f_R and reduced average V_T.

Histology

After the experiments animals were deeply anesthetized and then perfused transcardially with 4% of paraformaldehyde. After the perfusion, brains were removed and postfixed in the same fixative for 12-16 hours at 4°C. Brains were sectioned and stored in cryoprotectant solution.

Multiplex in situ hybridization was performed using RNAScope (Advanced Cell Diagnostics, Hayward, CA) according to the manufacturer's directions, briefly as follows.

This article is protected by copyright. All rights reserved.

Accepted Article

Sections were briefly washed in sterile phosphate buffered saline, mounted on charged slides and dried overnight. After 2 rinses in sterile water, sections were incubated with Protease IV (ACD) for 30 minutes at 42°C. Sections were rinsed twice in sterile water and incubated in RNAscope catalog oligonucleotide probes for *Nmb, Tyrosine Hydroxylase* (*Th*) *and Tryptophan hydroxlase* (*Tph*) transcripts for 2 hours at 40°C. After incubation with probes, tissue was treated according to the manufacturer's protocol (ACD). Slides were covered with Prolong Gold with DAPI Anti-fade mounting medium (Molecular Probes, Eugene, OR).

Cells were mapped and counted with a computer assisted stage controlled with the Neurolucida software (v. 11, MBF Bioscience, Colchester, VT) using a Zeiss AxioImager M2 after methods previously described (Stornetta et al. 2004). Digital photomicrographs using the same microscope were made with a Hamamatsu C11440 Orca-Flash 4.0LT digital camera. Filter settings for Atto 550, Alexa 488 or Atto 647 fluorophores were as follows: Alexa 488, excitation of 500 nm, emission of 535 nm; Atto 550, excitation of 545, emission of 605 nm; Atto 647, excitation of 640 nm, emission of 690 nm. Only cell profiles that included a nucleus were counted and/or mapped.

Statistics

For the statistical analysis we used GraphPad Prism (Version 7.03, La Jolla, CA, USA). Data were tested for normality using the D'Agostino and Pearson, Shapiro-Wilk or Kolmogorov-Smirnov's test. Data sets which failed all three tests were analyzed using non-parametric statistics. For normally distributed data, we used 1-way or 2-way ANOVA, usually with repeated measures, followed by Bonferroni's multiple comparisons test. The remainder of the data were analyzed using Kruskal-Wallis non-parametric test, followed by Dunn's *post hoc* multiple comparisons test. Normally distributed data were expressed as

This article is protected by copyright. All rights reserved.

Accepted Article

mean ± standard deviation (SD) and the rest as median ± 95% of confidence interval (CI). Differences were considered significant when $P<0.05$ but exact P values are reported. The relationship between the number of *Nmb* neurons and various physiological variables was tested with linear regression analysis followed by correlation analysis using Pearson's test. The relationship between hypercapnic ventilatory reflex and *Nmb* cells was modeled using various mathematical functions; a one-phase inverse exponential function provided the best fit.

RESULTS

Histology

Saline or SP-SAP was injected bilaterally into the RTN under electrophysiological guidance (3 microinjections per side; 0.6, 1.2 or 2.4 ng of toxin per injection). RTN neurons were identified histologically by the presence of *Nmb* transcripts (Shi *et al.*, 2017) (Fig. 1) and counted in a one-in-six series of transverse sections spanning the entire rostrocaudal extent of the nucleus. RTN *Nmb* cells were defined as those *Nmb* cells lying lateral to catecholamine cells (*Th* positive) or those under the facial motor nucleus in more rostral sections without *Th* cells present. The *Nmb* cell loss increased with the dose of toxin (Fig. 2A).

For physiological analysis, we regrouped the rats into three cohorts based on the number of *Nmb* RTN neurons identified post-mortem (Fig. 2B): saline-injected control rats (n=12; 359 ± 69 RTN *Nmb* neurons counted; range 273-478), mild lesion (ML) rats (n=12, 152 ± 92 RTN *Nmb* neurons remaining; range 78-374) and large-lesion (LL) rats (n=11, 29 ± 14 RTN *Nmb* neurons remaining; range 5-55). The mild lesion group included the 10 rats that

This article is protected by copyright. All rights reserved.

Accepted Article

had received the lowest dosage of toxin plus two rats, identified in Fig. 2A, that had a relatively small loss of *Nmb* neurons despite having received a higher toxin dose.

The number of serotonergic neurons located in the parapyramidal region and raphe magnus as well as the *Nmb* cells medial to the RTN ("midline" *Nmb*) were analyzed in a subset of 4 control and 4 LL rats (Fig. 1). No difference between control and lesion was noted between either of these sets of neurons (Figs. 1, 2). C1 adrenergic neurons were also counted from the same intact and RTN-lesion rats (Figs. 1, 2). Within the region examined, C1 cell numbers were significantly reduced by SSP-SAP, as noted in a prior study (Takakura *et al.*, 2008).

Baseline ventilatory parameters in normoxia

Resting respiratory frequency (f_R) was significantly elevated and tidal volume (V_T) significantly reduced in the LL group relative to control rats but V_E was unchanged (Table 1). In the ML group, f_R, V_T and V_E were similar to control rats. Resting mean arterial pressure was the same in the three rat cohorts (Table 1). Blood gases were not significantly different from control (n=11) in the ML (n=12) cohort (Fig. 3A-D). By contrast, in the LL (n=10) cohort, every parameter was significantly different from both control and ML rats (Fig. 3A-D). Specifically, PaO_2 was lower in the LL group than in controls (71.2 ± 6 *vs.* 79.6 ± 6 mmHg, P=0.0039), $PaCO_2$ was higher (48.5 ± 7 *vs.* 38.1 ± 3 mmHg, P<0.0001), the bicarbonate concentration was higher (34.6 ± 5 *vs.* 28.6 ± 2, P=0.0033) and arterial pH very slightly but yet significantly lower (7.46 ± 0.02 *vs.* 7.48 ± 0.01, P=0.0307). PaO_2 and $PaCO_2$

This article is protected by copyright. All rights reserved.

Accepted Article

were both highly correlated with the number of surviving RTN *Nmb* neurons (Fig. 3E, F), the first positively, the second negatively.

In summary, under normoxia, breathing parameters, blood gases and BP were normal in the rats with medium-sized lesions. The large lesion cohort also had a normal V_E but only because the reduction in V_T was offset by an increase in f_R. These rats were hypoxic (-8.4 mmHg difference relative to controls) and notably hypercapnic (+10.4 mmHg difference relative to controls) but their BP was normal.

Hypercapnic ventilatory reflex (HCVR) under hyperoxia

Representative examples of plethysmographic recordings from a control rat and one rat each selected from the mild or large lesion cohort are shown in Fig. 4B. At rest under normoxic conditions, and as described in Table 1, breathing frequency was higher in the LL group, V_T lower and V_E slightly but non-significantly reduced (Fig. 4C). Hyperoxia alone reduced f_R and V_E to a greater extent in the LL group than in the other two cohorts. Ventilation during exposure to CO_2 (FiO_2 maintained at 65% throughout) was much lower in the LL group relative to control or ML rats (Fig. 4C). The difference was highly significant for all three parameters (f_R, V_T, V_E) and at all levels of $FiCO_2$ (Fig. 4C). V_T and V_E were at control levels in the ML cohort under all gas environments but f_R was slightly reduced during hypercapnia. To quantify more precisely the HCVR we analyzed the change in f_R, V_T, V_E (Δf_R, ΔV_T, ΔV_E) elicited by raising $FiCO_2$ relative to the baseline values observed before CO_2 addition (65/0 point in Fig. 4C) (Fig. 5). ΔV_E elicited by 9% $FiCO_2$ in the LL cohort was reduced by 70.2 ± 14.6 % relative to the control rats (Fig. 5).

This article is protected by copyright. All rights reserved.

Accepted Article

Hyperoxia alone caused a much greater rise in $PaCO_2$ in the LL cohort (n=8) than in the control (n=7) rats (to 65.3 ± 9 *vs.* 47.1 ± 3 mmHg, P=0.0003; Fig. 5D); $PaCO_2$ also rose to a much higher level in the LL cohort than in the control rats after exposure to 9% $FiCO_2$ (to 102.1 ± 15 *vs.* 76.8 ± 3, P<0.0001; Fig. 5D). When expressed as $\Delta V_E / \Delta PaCO_2$ the HCVR was reduced by 72 ± 12 % in LL relative to the control rats.

The relationship between ΔV_E and the number of intact RTN *Nmb* neurons was best described by an inverse exponential function at all three levels of $FiCO_2$ (Fig. 5E). The ΔV_E of the two rats with the lowest ventilatory reflex was reduced by 91.8 ± 2 % relative to the average of the intact rats. These animals had only 5 and 17 *Nmb* neurons (3 ± 2 % of control values on average). Blood pressure was the same in all three rat groups, regardless of the $FiCO_2$ (Fig. 6A, B).

Oxygen consumption (VO_2) and CO_2 production (VCO_2) were measured in a separate cohort of 4 bilaterally lesioned rats (2.4 ng SSP-SAP) and 5 control rats. The hypercapnic ventilatory reflex of the lesioned rats was reduced to the same degree as the above described LL cohort but VO_2 and VCO_2 were not statistically different from the control rats (Table 2).

Cardiorespiratory response to poikilocapnic hypoxia is preserved after RTN lesions

Carotid body stimulation by hypoxia stimulates breathing; it also activates sympathetic tone which helps maintain BP constant. The hypoxic reflexes (ventilation and BP) were measured by exposing the rats to 15, 12 and 10% FiO_2 without supplemental CO_2 as summarized in Fig. 6A. Blood gases were measured twice: under normoxia and towards the

This article is protected by copyright. All rights reserved.

Accepted Article

end of the period of exposure to 10% FiO_2 (Fig. 7A, arrowheads). Breathing frequency (f_R), V_T and V_E were measured at the times indicated by the arrows in Fig. 7A. Representative examples of plethysmographic recordings from a control rat and one rat each selected from the mild or large-lesion cohort are shown in Fig. 7B. The changes in breathing parameters (Δf_R, ΔV_T and ΔV_E) relative to the normoxia baseline are shown in Fig. 7C. Δf_R was reduced in LL compared to control (values at FiO_2=10%, 42.8 ± 25 *vs.* 69.9 ± 22 breaths·min^{-1}, P=0.0096) but ΔV_T was larger (0.143 ± 0.14 *vs.* -0.065 ± 0.06 ml·100g^{-1}, P<0.0001). As a result ΔV_E was not significantly different between LL and control groups (34.1 ± 6 *vs.* 27.2 ± 8 ml·min·100g^{-1}, P=0.4382). Finally, the relationship between ΔV_E elicited by 10% FiO_2 and the number of surviving neurons did not reach statistical significance (P=0.06; Fig. 7E).

At rest under normoxia, BP and HR were the same in the three rat cohorts (Fig. 6, Table 1). The BP of intact rats decreased slightly and monotonically with increasing levels of hypoxia whereas it remained stable in the rats with large lesions of RTN neurons (Fig. 6C). The difference was highly significant. Heart rate tended to be slightly higher in the control rats (Fig. 6D); this difference could be baroreflex-related since the control rats tended to have lower BP. The blood gases of the three rat cohorts under hypoxia (FiO_2=10%) are shown in Table 3. No significant difference in $PaCO_2$ or PaO_2 were observed during hypoxia between the three groups. Thus RTN lesions had little impact on blood gas homeostasis under hypoxic conditions, unlike under hypercapnia.

Hypoxia-induced sighing after RTN lesions

Hypoxia also produces a prominent increase in the frequency of sighs (augmented breaths)(Ramirez, 2014). We examined the effect of RTN lesions on sighing because this

This article is protected by copyright. All rights reserved.

Accepted Article

behavior has been recently attributed to the activity of *Nmb*-expressing neurons, possibly located in the RTN region (Li *et al.*, 2016). A slight increase in sigh frequency was noted in the LL group both under normoxia and hyperoxia (Fig. 8). However, under hypoxia (15, 12 and 10% FiO_2) sigh frequency was essentially the same in all three rat groups except for a small reduction in the ML cohort under 10% FiO_2 (Fig. 8). The mean sigh frequency in normoxia, hyperoxia or hypoxia was about average in the LL group (Fig. 5). Sigh amplitude (i.e., V_T of sighs) was the same in all three groups of rats (LL: 1.87 ± 0.4; ML: 2.20 ± 0.3; Control: 1.94 ± 0.4 ml·100g^{-1}, 1-way ANOVA, P=0.0647).

Contribution of the carotid bodies to resting breathing is enhanced in rats with RTN lesions

To test the contribution of the carotid bodies to resting breathing, we subjected the rats to hyperoxia (65% FiO_2) according to the protocol shown in Fig. 9A. In intact unanesthetized mammals, hyperoxia produces a transient breathing reduction whose magnitude is used as an index of the contribution of the peripheral chemoreceptors to resting ventilation (Dejours, 1962). During longer term hyperoxia in Sprague-Dawley rats, breathing recovers to control levels, largely because RTN neurons are more active, presumably driven by an increase in local brain PCO_2 (Basting *et al.*, 2015).

Hyperoxia (65% FiO_2) had no detectable effect on any breathing parameter and at any time point in control rats (Fig. 9 B, C). f_R was higher under normoxia in the LL group than in the other two groups and lower early during hyperoxia (Fig. 9 C, left panel). V_T was lower at all times in the LL group. V_E was considerably lower in the LL rats both early and later during hyperoxia. The effect of hyperoxia on breathing parameters were further analyzed by measuring the changes (Δf_R, ΔV_T and ΔV_E) relative to the normoxia baseline (Fig. 10). RTN lesions, mild or large had no effect on ΔV_T (Fig. 10 B). Δf_R and ΔV_E were significantly

This article is protected by copyright. All rights reserved.

larger in the LL group than in control rats, but the values did not differ between the ML and control groups. $PaCO_2$ was significantly larger under normoxia in the LL group (see also Table 1).

The protocol was re-run after catheter implantation in a large subset of the rats (n=7 from each cohort) to examine the effects of hyperoxia on blood gases. After 20 min of hyperoxia, $PaCO_2$ of the control and ML rats was identical and only mildly elevated relative to normoxia (control: from 39.2 ± 2 to 46.6 ± 3 mmHg, P=0.006; n=7; ML rats: from 38.6 ± 3 to 45.1 ± 9 mmHg, P=0.0174, n=7). In the LL rats $PaCO_2$ (n=8) was already significantly higher than that of control rats under hypoxia, and rose to a much higher level still under hyperoxia (from 50.6 ± 5 to 74.4 ± 11 mmHg, P<0.0001, n=8; Fig. 10D). The higher increase in $PaCO_2$ during hyperoxia in LL rats indicates that these rats presented a dramatic alveolar hypoventilation during hyperoxia compared to control. The early and sustained reduction in minute-ventilation (ΔV_E) produced by hyperoxia was highly correlated with the loss of *Nmb* neurons (Fig. 10 E, F).

Sleep-related changes in breathing pattern are preserved after RTN lesions

RTN hypoplasia or outright developmental failure is suspected to occur in congenital central hypoventilation syndrome (CCHS), a disease caused by *Phox2b* mutations (Amiel *et al.*, 2003; Amiel *et al.*, 2009; Weese-Mayer *et al.*, 2010). CCHS is characterized by severe hypoventilation or even complete apnea during slow-wave sleep while ventilation improves during REM sleep. We already know that, in intact rats, RTN activity is a major determinant of ventilation during slow-wave sleep whereas the contribution of this nucleus is much reduced during REM sleep (Burke *et al.*, 2015a). The goal of this next series of experiments

This article is protected by copyright. All rights reserved.

Accepted Article

Accepted Article

was to test whether ventilation is depressed to a much greater degree during SWS than during REM sleep in animals with extensive RTN lesions.

REM sleep episodes were identified by a combination of posture, neck muscle atonia, theta (6-7Hz) cortical rhythm, and increased variability of breathing frequency and amplitude (Fig.11A). Slow-wave sleep was identified by large amplitude low frequency EEG, low amplitude neck EMG and extreme breathing regularity, and periods of quiet waking by higher amplitude neck EMG but lack of movement, desynchronized EEG and regular breathing (Fig. 11). Episodes of REM and slow-wave sleep occurred in all groups of rats. We did not quantify the proportion of time spent in each state. f_R, V_T and V_E were averaged during episodes of REM sleep (1-3 min per rat) and compared to values recorded during SWS or quiet waking (3-4 min per rat). A single numerical value representing the mean f_R, V_T and V_E during each of the three states was generated per rat. The results were analyzed by 2-way ANOVA (factors: sleep stage and extent of lesions). There was a significant effect of both sleep stage and the extent of the RTN lesions on all breathing parameters but no interaction between the two factors (2-way RM ANOVA; Fig. 11). This result indicates that the effect of sleep stages on breathing parameters were preserved in rats with RTN lesions (i.e. during REM sleep f_R increased, V_T decrease and V_E remained the same relative to SWS) and V_T was reduced to approximately the same extent during wake, SWS and REM sleep.

We also examined whether rats with RTN lesions exhibited breathing instability during slow-wave sleep. Breathing variability was measured by the coefficient of variation (CV) of the breathing period. In intact rats, CV was lowest during slow wave sleep and highest during REM sleep, as expected (Fig. 12 D). RTN lesions had no effect on this pattern (2-way RM ANOVA; Fig. 12D). In sum, the hypothesis that RTN lesions would cause apneas or at least much more severe hypoventilation during SWS than during quiet waking or REM sleep was not supported by the experimental data.

This article is protected by copyright. All rights reserved.

Accepted Article

Ventilation under hyperoxia and during slow-wave sleep

The preceding experiments were conducted in rats breathing room air. The results (vigilance state-independent effect of RTN lesions on breathing parameters) could mean that, in animals with RTN lesions, breathing is maintained by the carotid bodies to an equivalent degree during both waking and slow-wave sleep. To test this hypothesis we measured ventilation during slow-wave sleep and quiet waking in control (n=10) and rats with RTN lesions (LL group; n=11) given 65% FiO_2 to minimize the contribution of the carotid bodies. The data come from the hyperoxia experiments described above (Figs. 9 and 10) but we analyzed episodes of SWS and quiet waking separately. Because hyperoxia was only maintained for 20 min, episodes of REM sleep were not frequent enough to enable us to analyze breathing during this stage.

Under hyperoxia, V_E was reduced to the same extent (~40%) in rats with RTN lesions during quiet waking (LL rats, 24.0 ± 4; control rats, 40.6 ± 8 $ml \cdot min \cdot 100g^{-1}$, $P<0.0001$) and SWS (19.2 ± 4 *vs.* 33.7 ± 6 $ml \cdot min \cdot 100g^{-1}$, $P<0.0001$). As under normoxia, there was a significant effect of both state of vigilance and RTN lesions on all ventilatory parameters but no interaction between these factors (2-way RM ANOVA; Fig. 12A-C). V_E was definitely lowest in sleeping rats with RTN lesions breathing 65% FiO_2 than under any other conditions examined but apnea was still not observed. During hyperoxia, breathing variability was increased in rats with large RTN lesions compared to controls (Fig. 12E) although the difference reached statistical significance only during the awake state.

This article is protected by copyright. All rights reserved.

Accepted Article

DISCUSSION

To date, this study is the most comprehensive description of the cardiorespiratory consequences of an almost complete destruction of RTN neurons in adult rodents. RTN lesions reduced the CRC by up to 92% and produced a degree of hypercapnia and hypoxia at rest that increased with the severity of the lesion. At rest, rats with a near-complete lesion of the RTN had a similar V_E to control rats because a reduction in V_T was offset by an increase in f_R. However, the combination of increased $PaCO_2$ and unchanged CO_2 production at rest in rats with RTN lesions indicates that alveolar ventilation was severely reduced compared to controls, likely due to increased physiological dead space. RTN lesions did not fully phenocopy the breathing deficits observed in congenital central hypoventilation syndrome. While the CRC was massively decreased, the other cardinal sign of the disease, sleep apnea, was not reproduced. The following discussion focuses on the differences between rats with an intact RTN and those with large lesions of this nucleus because intermediate size lesions had virtually no effect.

Histology

RTN *Nmb* neurons express neurokinin-1 receptors (*tacr*) (Shi *et al.*, 2017), which presumably accounts for their vulnerability to SSP-SAP (Wiley & Lappi, 1999; Nattie & Li, 2002b). The toxin partially damaged the rostral-most C1 neurons, whose processes are intermingled with RTN neurons (Stornetta *et al.*, 2006). However, the bulk of the C1 neurons reside caudal to RTN; these neurons seemed intact. The serotonergic neurons located within the parapyramidal region and the raphe (magnus and pallidus), some of which contribute to the hypercapnic ventilatory reflex (Brust *et al.*, 2014; Hennessy *et al.*, 2017), were unaffected as were the Phox2b-negative (non-RTN) *Nmb* neurons located in the ventromedial medulla

This article is protected by copyright. All rights reserved.

Accepted Article

(Shi *et al.*, 2017). Damage to the very rostral portion of the ventral respiratory column (Bötzinger region) was not immediately apparent but could not be objectively evaluated with the present histological analysis. Although NK1R-rich regions of the respiratory column such as the preBötzinger complex innervate the RTN region (Tan *et al.*, 2010), SSP-SAP is not known to destroy respiratory neurons in a retrograde manner (Takakura *et al.*, 2008; 2014). The general region that we targeted also harbors neurons known as the parafacial expiratory oscillator (Huckstepp *et al.*, 2015; 2016). This entity has not yet been identified histochemically and could conceivably be a subset of RTN neurons that regulate active expiration preferentially (Marina *et al.*, 2010; Burke *et al.*, 2015a)

In short, the toxin destroyed a very large percentage of RTN *Nmb* neurons while sparing nearby serotonergic, and *Nmb* neurons located in the ventromedial medulla. The rostral C1 catecholaminergic neurons were partially damaged. The parafacial expiratory oscillator is not identifiable yet; its fate could not be determined.

RTN lesions reduce alveolar ventilation at rest under normoxia despite a compensatory increase in carotid body drive to breathe

Arterial pH was minimally changed by RTN lesions, consistent with the well-established primacy of the kidneys for long-term pH control. Also as anticipated, an increase in plasma bicarbonate contributed to the restoration of arterial pH to its normal level. However, after near complete RTN lesions, $PaCO_2$ was notably elevated (48 *vs.* 38 mmHg) and PaO_2 reduced.

This article is protected by copyright. All rights reserved.

Accepted Article

Based on the classic relationship between $PaCO_2$, VCO_2 and alveolar ventilation (V_A) ($PaCO_2=k\cdot VCO_2/V_A$) and the fact that VCO_2 was unchanged, we conclude that large RTN lesions reduced alveolar ventilation by 21% on average. Such severe hypoventilation occurred at rest despite the fact that V_E was unchanged. After lesion, V_E was far more dependent on the carotid bodies in lesioned than intact rats given the much greater V_E reduction elicited by hyperoxia. Although, V_E was unchanged after RTN lesions, V_T was reduced and f_R was increased. That V_E depended predominantly on f_R after RTN lesions suggests that the primary cause of the alveolar hypoventilation could be an increase in the physiological dead space.

RTN lesions virtually eliminate the CRC

The HCVR measured under hyperoxia (hyperoxic HCVR) overestimates the contribution of central chemoreceptors because the carotid bodies can still be activated by hypercapnia (Pepper *et al.*, 1995). This overestimation could be larger after RTN lesions because arterial PCO_2 rises higher than in intact rats when they breathe a CO_2-enriched mixture.

The f_R and V_T components of the hyperoxic HCVR were both reduced by RTN lesions, consistent with prior evidence that these neurons regulate both variables (Abbott *et al.*, 2011; Basting *et al.*, 2015). The relationship between the hyperoxic HCVR and the number of surviving RTN *Nmb* neurons was an inverse exponential function. A 57.6 ± 26 % kill rate (ML rats) produced virtually no effect. The LL cohort had a 70.2 ± 16.6 % reduction of the hyperoxic HCVR and 8 ± 4 % of *Nmb* RTN neurons remaining. The two rats with the

This article is protected by copyright. All rights reserved.

Accepted Article

most extreme RTN lesions (only 3 ± 2 % *Nmb* neurons left) had a 92 % reduced hyperoxic HCVR.

Based on these results, RTN neurons may mediate more than 92% of the CRC since some of the residual HCVR was likely driven by the carotid bodies. That only 10% of the hyperoxic HCVR would be mediated by the carotid bodies seems *a priori* to contradict prior observations (Rodman *et al.*, 2001). However, the contribution of the carotid bodies to the HCVR is probably smaller in Sprague-Dawley rats than in dogs (Mouradian *et al.*, 2012). In addition, a portion of the peripheral chemoreflex is normally mediated by the RTN, therefore this portion of the reflex would be eliminated after this nucleus is destroyed (Takakura *et al.*, 2006).

The prenatal loss of RTN neurons by conditional expression of a mutated form of *Phox2b* (*Phox2b* ^{27ala}) eliminates only 60% of the HCVR of adult mice (Ramanantsoa *et al.*, 2011) but the HCVR was measured under normoxia and the 40% residual reflex could also have been largely mediated by the peripheral chemoreceptors. Indeed these authors showed that at least at P4, hyperoxia (100% O_2) produced considerable hypoventilation in these mutant mice. The hyperoxic HCVR of mice with combined *Gpr4* and *Task-2* genomic deletion, which eliminates the ability of RTN neurons to respond to acidification, is also 90% reduced. In short, RTN destruction or selective deletion of its ability to respond to acid virtually eliminates the CRC in rodents. These observations need to be reconciled with the large body of evidence which supports the existence of multiple additional central respiratory chemoreceptors, (locus coeruleus, serotonergic neurons, orexinergic neurons, nucleus solitary tract, ventral respiratory column, etc.). A tempting hypothesis is that serotonin, noradrenaline and orexin neurons regulate the CRC via their excitatory projections to the RTN (Mulkey *et al.*, 2007; Lazarenko *et al.*, 2011; Hawryluk *et al.*, 2012; Brust *et al.*, 2014; Oliveira *et al.*,

This article is protected by copyright. All rights reserved.

Accepted Article

2016). These neurons could also amplify the effect of a given change in RTN neuron discharge by enhancing the excitability of the respiratory pattern generator (Viemari & Ramirez, 2006; Ptak *et al.*, 2009). The previously proposed existence of chemoreceptors distributed throughout the ventral respiratory column and nucleus of the solitary tract (Solomon *et al.*, 2000; Conrad *et al.*, 2009) is more difficult to reconcile with the magnitude of the CRC reduction elicited by RTN lesions, unless one postulates that all these neurons also operate via the RTN. The view that these neurons are respiratory chemoreceptors relies on the observation that focal brain acidification *in vivo* activates breathing and/or that acidification depolarizes neurons and or astrocytes in slices (Gourine & Kasparov, 2011; Nattie, 2012). The possibility that these are non-specific actions of pH cannot be excluded.

RTN lesions have considerable functional selectivity; locomotion, posture, grooming, state-dependency of breathing, resting blood pressure and heart rate were not detectably altered. As discussed below, the hypoxic ventilatory response tended to be enhanced rather than decreased by RTN lesions. This functional selectivity does not signify nor presuppose that the lesions were totally selective for *Nmb* neurons. A huge percentage of *Nmb* cells need to be destroyed to produce a detectable loss of the physiological function governed by these neurons. The same principle likely applies to neurons located at the immediate periphery of the RTN; the loss of a small percentage is presumably of little physiological consequence. The C1 cells are a case in point as discussed below.

The cardiovascular and respiratory components of the peripheral chemoreflex are preserved or enhanced by RTN lesions.

The cardiorespiratory stimulation elicited by moderate and short-term hypoxia is caused by the activation of the carotid bodies (Kumar & Prabhakar, 2012). The persistence of

This article is protected by copyright. All rights reserved.

the hypoxic ventilatory reflex in toxin-treated rats suggest that the toxin did not damage the respiratory pattern generator or that the damage was slight.

The hypoxic ventilatory response was qualitatively altered by RTN lesions; specifically, the frequency response was attenuated and the tidal volume component enhanced. The f_R increase could have been reduced simply because this parameter has a finite dynamic range and it was already elevated under normoxia. Also, hypoxia inhibits the RTN via alkalosis (Basting *et al.*, 2015) which normally opposes the direct breathing stimulation elicited by the RTN-independent effect of carotid body stimulation on the respiratory pattern generator (Guyenet *et al.*, 2017). Such disfacilitation would not occur in the absence of RTN neurons and the full effect of the carotid bodies on tidal volume may therefore be revealed.

Resting BP was unaffected by the lesions, consistent with the minimal effects of the toxin on C1 cells and the raphe. C1 neurons are profoundly activated by carotid body stimulation (Sun & Reis, 1993) probably by second-order chemoreceptor neurons located in the nucleus of the solitary tract (Koshiya *et al.*, 1993; Aicher *et al.*, 1996; Dempsey *et al.*, 2017). This activation increases sympathetic tone, which minimizes hypotension under hypoxic conditions (Burke *et al.*, 2014; Wenker *et al.*, 2017). Interestingly, BP was better maintained during hypoxia in rats with RTN lesions than in intact animals. The simplest explanation is the already evoked enhancement of the hypoxic reflex but there are others. The rostral bulbospinal C1 cells are also a convergence point of the peripheral and central components of the sympathetic chemoreflex (Sun & Reis, 1994; Moreira *et al.*, 2006). RTN neurons could conceivably mediate the cardiovascular effects of a rise in CNS PCO_2 since they appear to innervate C1 neurons (Dempsey *et al.*, 2017). As the RTN is silenced by hypoxia (Basting *et al.*, 2015), the contribution of this nucleus to the discharge of the C1 cells should be reduced during hypoxia thereby lessening the ability of these neurons to preserve

This article is protected by copyright. All rights reserved.

Accepted Article

BP homeostasis. In the absence of RTN neurons, the direct excitatory effect of the carotid bodies on the C1 cells should be unopposed by the loss of excitatory input from the RTN and BP should therefore be better maintained, as was observed.

In intact normocapnic rats, RTN neurons are activated by carotid body stimulation, suggesting that activation of the RTN contributes to the peripheral chemoreflex (Takakura *et al.*, 2006). However, hypoxia increases ventilation while silencing the RTN, which suggests that carotid body stimulation can also activate the respiratory pattern generator via an RTN-independent pathway (Basting *et al.*, 2015). The persistence of the peripheral chemoreflex after near complete lesions of the RTN provides additional evidence for the existence of such a pathway.

The selectivity of RTN lesions towards the central component of the chemoreflex is by no means unique. Genetic deletion of serotonergic neurons or destruction of the locus coeruleus also produces substantial reductions of the CRC without reducing the hypoxic ventilatory response (Hodges *et al.*, 2008; Gargaglioni *et al.*, 2010). This suggests that the CRC is far more dependent on the level of activity of wake-promoting neurons than the peripheral chemoreflex. This speculation is consistent with the strong excitatory effects of serotonin, noradrenaline and orexin on RTN neurons (Lazarenko *et al.*, 2011; Hawryluk *et al.*, 2012; Kuo *et al.*, 2016). The carotid bodies are the first line of defense against hypoventilation. The relative independence of this reflex from the activity of wake promoting modulators may have survival value.

Accepted Article

This article is protected by copyright. All rights reserved.

Accepted Article

Loss of RTN Nmb neurons reduces neither the frequency nor the amplitude of hypoxia-induced sighs.

Hypoxia and arousal are the most common triggers of sighs (Ramirez, 2014). Even almost total elimination of RTN *Nmb* neurons did not change sigh frequency in rats exposed to hypoxia. This negative outcome is consistent with prior evidence that optogenetic stimulation of RTN neurons does not produce sighs in awake rats (Burke *et al.*, 2015b) and that RTN neurons are typically silenced by alkalosis, a normal consequence of hypoxia (Basting *et al.*, 2015). Moreover, RTN neurons are typically excited by hypercapnia/acidosis, a stimulus that reduces hypoxia-induced sigh incidence (Mulkey *et al.*, 2004; Bell *et al.*, 2009).

Importantly, sigh amplitude was also unaffected by RTN lesions. A non-specific impairment of the motor command to inspiratory muscles or a defect of muscle contractility is therefore unlikely to explain the inability of hypercapnia to increase V_T after RTN lesions. Since the hypoxic ventilatory reflex and sighing are both preserved, the most likely interpretation is that RTN lesions abrogate preferentially the CO_2-regulated excitatory drive to the pattern generator.

While our data do not support the view that RTN *Nmb* neurons trigger sighs, they do not entirely rule it out either. A small subset of RTN *Nmb* neurons may not be activated by hypercapnia (Shi *et al.*, 2017) and could be those that regulate sighing (Li *et al.*, 2016). These neurons could conceivably be selectively resistant to SSP-SAP.

This article is protected by copyright. All rights reserved.

Accepted Article

RTN lesions do not cause sleep apnea, even under hyperoxia

We did not find any interaction between resting breathing parameters and the state of vigilance after RTN lesions. In other words, breathing parameters were proportionally changed during waking, slow-wave sleep and REM sleep in rats with RTN lesions compared to intact rats. The presumption, still unconfirmed by histopathology, is that the RTN is hypomorphic or fails to develop altogether in congenital central hypoventilation syndrome (CCHS)(Amiel *et al.*, 2003; Dubreuil *et al.*, 2008; Weese-Mayer *et al.*, 2010). Based on the present results, the absence of the RTN could underlie much of the reduced hypercapnic ventilatory reflex of CCHS patients but it does not explain the severity of the hypoventilation present during slow-wave sleep (Weese-Mayer *et al.*, 2010).

Phox2b mutations in humans also impair the peripheral chemoreflex to varying degrees (Perez & Keens, 2013; Carroll *et al.*, 2014). *Phox2b* mutations have the potential of interfering with the development of the carotid bodies, the nucleus of the solitary tract and brainstem catecholaminergic neurons, all of which contribute to this reflex (Dauger *et al.*, 2003; Stornetta *et al.*, 2006; Goridis *et al.*, 2010; Nobuta *et al.*, 2015; Malheiros-Lima *et al.*, 2017). The combination of a weak peripheral chemoreflex and a lack of RTN neurons may be required to cause severe hypoventilation during slow-wave sleep in CCHS patients. Indeed, in rats with large RTN lesions, hypoventilation was most pronounced when the animals were both in slow-wave sleep and under hyperoxia. Yet, even under these conditions, breathing remained regular and sleep apnea was not observed. In short, the combination of large RTN lesions and hyperoxia did not produce sleep apnea and therefore did not phenocopy the breathing disorder experienced by severely affected CCHS patients.

This article is protected by copyright. All rights reserved.

Accepted Article

Similarities and differences between the effects of genetic (Phox2b^{27alacki}; Egr-2^{cre} mice) *and toxin-induced lesions of the RTN*

Although the genetic lesions of the RTN were in mice (Ramanantsoa *et al.*, 2011) and the toxin-based lesions in rats, the resulting effects have some striking similarities. In both models, the animals survive the lesions, the CRC is greatly reduced, the HVR is preserved, resting V_E under normoxia is not significant changed and the contribution of the carotid bodies to breathing is enhanced. However, there are also notable differences between these models. The arterial PCO_2 set-point is increased in rats with toxin-based lesions whereas this parameter does not change in mice (Ramanantsoa *et al.*, 2011). Although procedural details varied with respect to how the arterial blood gases were sampled, the absence of hypercapnia in adult *Phox2b^{27alacki}; Egr-2^{cre}* mice is consistent with the fact that neither V_T nor f_R were altered at rest, unlike in the rat model. Another difference is that the HCVR of *Phox2b^{27alacki}; Egr-2^{cre}* mice recovered to 40% of control in adulthood whereas, in toxin-lesioned rats, we observed up to 90% reduction of this reflex. This difference could be methodological: we measured the HCVR under hyperoxic conditions to minimize the contribution of the carotid bodies whereas the reflex was measured under normoxia in mice. Finally, unlike the *Phox2b^{27alacki}; Egr-2^{cre}* mice, rats with RTN lesions had a regular breathing rate without apnea, even during sleep.

In summary, genetic lesions of RTN in mice produce breathing deficits that are similar but not identical to those observed after SSP-SAP lesions in adult rats. A persistent hypoventilation occurs when the RTN is lesioned in adult rats and the CRC deficit may be more extreme. These differences could be species-related. Alternately, interfering with RTN development could trigger more efficient countervailing changes than when RTN lesions are performed in adults.

This article is protected by copyright. All rights reserved.

Accepted Article

Experimental limitations and additional caveats

We did not destroy the RTN completely. In the LL cohort we still identified 29 ± 14 RTN neurons in one–in–six series of histological sections (estimated 92 ± 4 % reduction). Given the distinctly non-linear relationship existing between the chemoreflex deficit and the size of the lesions, the full contribution of the RTN to the CRC and the importance of this nucleus to maintain breathing during slow wave sleep has probably been underestimated.

Nmb neurons may not respond equally to hypercapnia as judged by Fos expression (Shi *et al.*, 2017), therefore their contribution to the central respiratory chemoreflex could also be variable. This could explain some of the variability between the percentage of *Nmb* neurons destroyed and the magnitude of the chemoreflex deficit.

The breathing deficits that we observed could have resulted, at least partly, from the loss of parafacial neurons other than *Nmb* neurons. The validity of our interpretations will require confirmation using even more selective lesions of the *Nmb* neurons. Also, the physiological experiments were conducted 3-4 weeks after injection of the toxin. This delay may not have been sufficient for all compensatory mechanisms (sprouting of surviving neurons) to have reached a steady-state.

CONCLUSIONS

Based on the present results, at least 90% of the CRC is mediated via activation of RTN neurons which can likely be identified by the presence of *Nmb* transcripts. Near complete destruction of RTN in adult rats is survivable as is the congenital absence of this

This article is protected by copyright. All rights reserved.

nucleus in mice. Arterial pH is virtually unaffected by RTN lesions but arterial PCO_2 is elevated significantly at rest.

In the absence of the RTN, V_T and f_R can still be vigorously activated by carotid body stimulation and sighs of normal amplitude are elicited by hypoxia. Thus, in quietly resting animals, the RTN seems to selectively mediate the bulk of the breathing stimulation evoked by a rise in CNS PCO_2 (Guyenet *et al.*, 2017).

Despite an increased contribution of the carotid bodies to breathing, also noted by previous investigators (Ramanantsoa *et al.*, 2011; Takakura *et al.*, 2014), RTN lesions cause significant alveolar hypoventilation. The integrity of central chemoreceptors is therefore required to maintain normal alveolar ventilation at rest. The integrity of the peripheral chemoreceptors is equally important in that respect, especially in large species, in which peripheral chemoreceptor denervation produces very long-lasting and virtually irreversible (humans) or only partially and slowly reversible hypoventilation (Rodman *et al.*, 2001; Smith *et al.*, 2006).

RTN lesions in adult rats do not reproduce exactly the breathing deficits observed in mice in which the absence of this nucleus is caused by conditional expression of *Phox2b*^{27ala}. Moreover, neither model phenocopies the congenital central hypoventilation syndrome exactly. The most obvious missing trait is sleep apnea. This sign of CCHS likely results from additional neuronal abnormalities besides the loss of the RTN.

Accepted Article

This article is protected by copyright. All rights reserved.

Accepted Article

Tables

Table 1. *Resting cardiorespiratory parameters in control and rats with RTN lesions.*

	Control	ML	LL	*P* value*
n	12	12	11	
f_R (breaths·min^{-1})	74 ± 11	74 ± 6	87 ± 14*#	0.0328
V_T (ml·100g^{-1})	0.45 ± 0.06	0.50 ± 0.1	0.32 ± 0.08*#	0.0019
V_E (ml·min·100g^{-1})	33.2 ± 5.7	37.4 ± 7.9	27.2 ± 6.3#	0.1215
n	9	9	9	
BP (mmHg)	111 ± 9	112 ± 9	111 ± 4	>0.9999
HR (mmHg)	358 ± 26	358 ± 25	341 ± 25	0.5050

Legend: ML, mild lesion; LL, Large lesion; BP, blood pressure; HR, heart rate. Statistical analysis by one-way ANOVA with Bonferroni's post-test. There was an overall effect of the extent of RTN lesions on f_R (P=0.0125); Bonferroni's post-test for f_R: *Control *vs.* LL, P=0.0287; #ML *vs*. LL, P=0.0210). There was also an overall effect of lesion on V_T (P<0.0001); Bonferroni's post-test for V_T:*Control *vs.* LL, P=0.0019; ML *vs.* LL, P<0.0001. There was an overall effect of extent of the lesions on V_E (P=0.0042). Bonferroni's post-test: #ML *vs.* LL, P=0.0032. There was no overall effect of extent of the lesions on resting BP (P=0.9226) and HR (P=0.2682).

This article is protected by copyright. All rights reserved.

Accepted Article

Table 2. *Resting metabolic parameters in RTN lesion rats and control*

	Control	SP-SAP (2.4 ng)	*P* value
n	5	4	
VO_2 ($ml \cdot min^{-1} \cdot 100g^{-1}$)	2.1 ± 0.18	1.9 ± 0.21	0.1886
VCO_2 ($ml \cdot min^{-1} \cdot 100g^{-1}$)	1.8 ± 0.18	1.6 ± 0.19	0.1111
Resting V_E ($ml \cdot min^{-1} \cdot 100g^{-1}$)	30.0 ± 4.0	24.1 ± 5.8	0.1136
Hypercapnic V_E ($ml \cdot min^{-1} \cdot 100g^{-1}$)	73.3 ± 10.6	39.7 ± 28.4 *	0.0426

Legend: VO_2, oxygen consumption; VCO_2, CO_2 production; Resting V_E, minute-volume in normoxia, normocapnia; Hypercapnic V_E, minute-volume measured in hypercapnia ($FiCO_2$=6%) in a hyperoxia background (FiO_2=65%). *Different from control.

Table 3. *Blood gases of control and rats with RTN lesions exposed to hypoxia (FiO_2=10%)*

	Control	ML	LL	*P* value
n	5	7	8	
pH	7.63 ± 0.03	7.61 ± 0.03	7.68 ± 0.02*#	0.0065
$PaCO_2$ (mmHg)	22.5 ± 1.5	22.7 ± 3.0	22.1 ± 2.1	>0.9999
PaO_2 (mmHg)	31.6 ± 1.5	32.4 ± 2.5	33.8 ± 1.7	0.2321
$HCO3^-$ ($mmol \cdot l^{-1}$)	23.8 ± 1.7	23.0 ± 3.5	26.1 ± 2.3	0.4853

Legend: ML, mild lesion; LL, Large lesion; BP, blood pressure; HR, heart rate. Statistical analysis by one-way ANOVA and Bonferroni's post-test. There was an overall effect of extent of the RTN lesion on blood pH during hypoxia (P=0.0001). Bonferroni's post-test: *Control *vs*. LL, P=0.0065; #ML *vs.* LL, P=0.0001. There was no overall effect of RTN lesions on $PaCO_2$ (P=0.8849), PaO_2 (P=0.1792) or $HCO3^-$ (P=0.1021) during hypoxia.

This article is protected by copyright. All rights reserved.

Figure legends

Figure 1: [Sar^9, Met $(O_2)^{11}$]-substance P *(SSP-SAP) destroys RTN Neuromedin B (Nmb) neurons, reduces C1 (tyrosine hydroxylase, Th) neurons and spares medial medullary serotonin (tryptophan hydroxylase, Tph) and Nmb neurons.*

A, B. Photomicrographs of approximately the same level of transverse cut ventral medulla from control (A) or SSP-SAP large lesion rats (B). Midline is towards the right, dorsal towards the top and ventral surface shown at the bottom. Sections were treated with RNAScope for multiplex fluorescent in situ hybridization; *Nmb* transcripts are shown in magenta, *Th* transcripts are in blue and *Tph* transcripts are in green. Scale bar in B=250 μm, applies to both A and B.

C, D. Drawings of 9 transverse sections from approximately 12 to 10 mm behind bregma encompassing the entirety of the RTN collapsed into one plane showing the distribution of transcripts for RTN *Nmb* (dark magenta circles), non-RTN *Nmb* ("midline" *Nmb*, yellow squares), *Th* (orange diamonds) and *Tph* (green triangles). C is from the same animal shown in A where D is from the same animal shown in B. Scale in C=1 mm, applies to C and D.

E, F. Photomicrographs from the same animals shown in A and B respectively showing the separation of RTN *Nmb* neurons from C1 (*Th*) neurons and midline *Nmb* (non RTN neurons) as well as the different size and shape of these classes of *Nmb* neurons in the insets surrounded by dotted lines. *Th* transcripts shown in blue, *Nmb* transcripts in magenta. Scale in E=200 μm for main part of E and F or 15 μm for the top inset and 25 μm for the lower inset in E.

Accepted Article

This article is protected by copyright. All rights reserved.

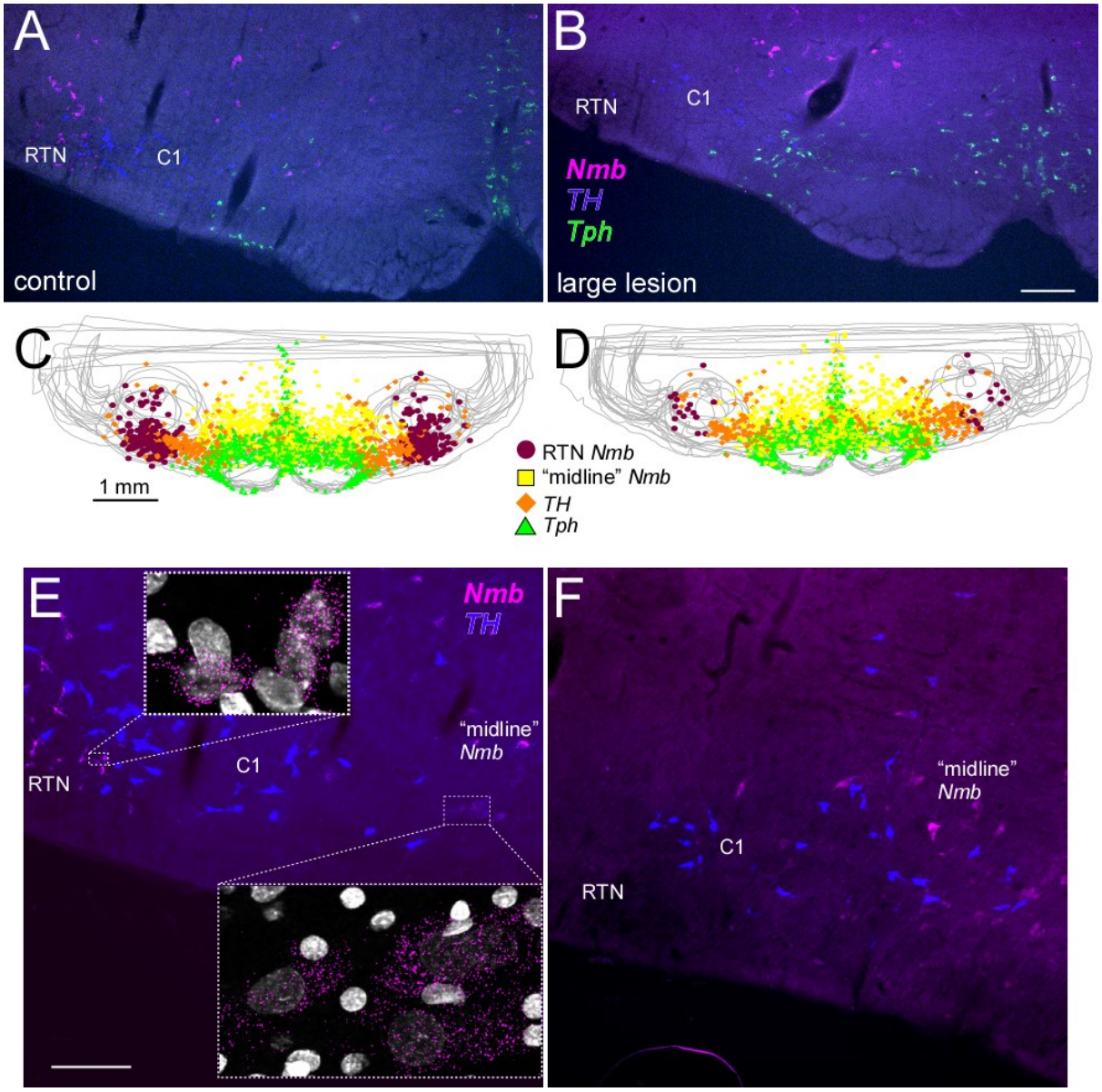

Accepted Article

This article is protected by copyright. All rights reserved.

Figure 2: *Number of Nmb, Th and Tph neurons in SSP-SAP injected rats and control.*

A. Effect of dose of SSP-SAP on number of *Nmb* neurons. There was an overall effect of the dose (P<0.0001, Kruskall-Wallis). Dunn's post-test: * Control *vs.* SSP-SAP (1.2 ng, P=0.0012) and Control *vs*. SSP-SP (2.4 ng, P<0.0001).

B. Number of *Nmb* neurons after posthoc regroupment of lesioned rats into two groups according to lesion size. There was an overall effect of the lesion size [F (2, 32) =70.1; P<0.0001]. Bonferroni's post-test: * Control *vs.* Mild lesion (P<0.0001), Control *vs.* Large lesion (P<0.0001), # Mild lesion *vs.* Large lesion (P=0.0004).

C. Number of *Th* neurons in the large lesion group (n=4) compared to control (n=4). There was a significant reduction of *Th* neurons on the large lesion group compared to control (* Control *vs.* Large lesion, P=0.0286, Mann-Whitney).

D. Number of midline *Nmb* neurons in the large lesion group (n=4) compared to control (n=4). There was no significant differences between the number of midline *Nmb* neurons of large lesion compared to control (P=0.7943, Unpaired t test).

E. Number of *Tph* neurons in the large lesion group (n=4) compared to control (n=4). There was no significant differences between the number of *Tph* neurons of large lesion compared to control (P=0.4055, Unpaired t test).

Accepted Article

This article is protected by copyright. All rights reserved.

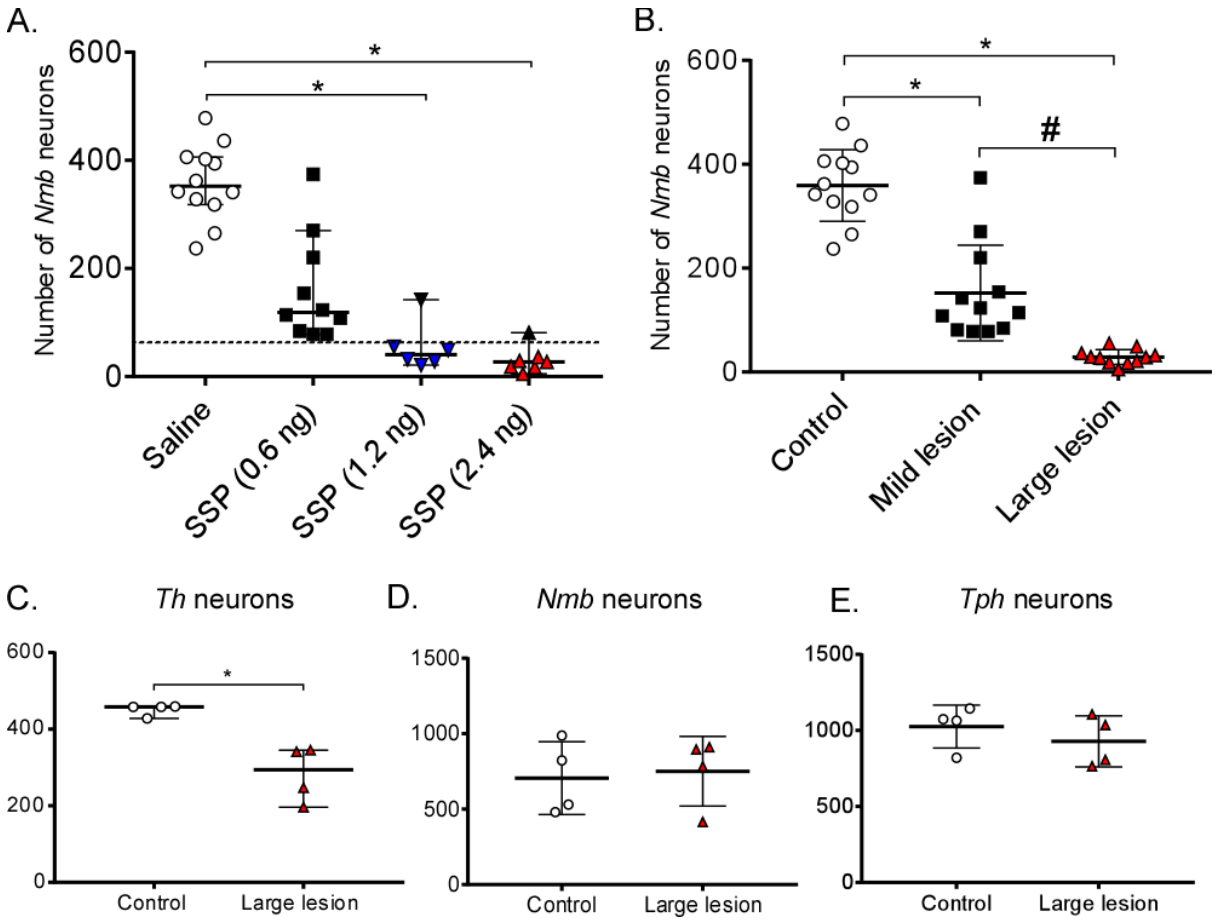

Accepted Article

This article is protected by copyright. All rights reserved.

Figure 3: *Blood gases under normoxia in intact vs. RTN-lesioned rats*

A. Arterial PCO_2 in control rats (C), rats with mild (ML) or large (LL) lesions of RTN. One-way ANOVA [F (2, 30) = 15.7; P<0.0001]. Bonferroni's multiple comparison test: *, P < 0.0001; #, P < 0.0001.

B. Arterial PO_2 in control rats (C), rats with mild (ML) or large (LL) lesions of RTN. One-way ANOVA [F (2, 30) = 7.6; P=0.0021]. Bonferroni's multiple comparison test: *, P=0.0042; #, P < 0.0074.

C. Arterial pH in control rats (C), rats with mild (ML) or large (LL) lesions of RTN. One-way ANOVA [F (2, 30) = 5.19; P=0.0116]. Bonferroni's multiple comparison test: *, P=0.0464; #, P=0.0154.

D. Plasma bicarbonate in control rats (C), rats with mild (ML) or large (LL) lesions of RTN. Kruskall-Wallis test (P=0.0018). Dunn's multiple comparison test: *, P=0.0033; #, P=0.0102.

E. Correlation between the number of *Nmb* neurons and $PaCO_2$. There was a significant correlation between the number of *Nmb* neurons and the arterial PCO_2 (P=0.0048, Pearson r = -0.4788).

F. Correlation between the number of *Nmb* neurons and resting PaO_2. There was a significant correlation between the number of *Nmb* neurons and the PaO_2 (P=0.0082, Pearson's r = 0.4522).

Accepted Article

This article is protected by copyright. All rights reserved.

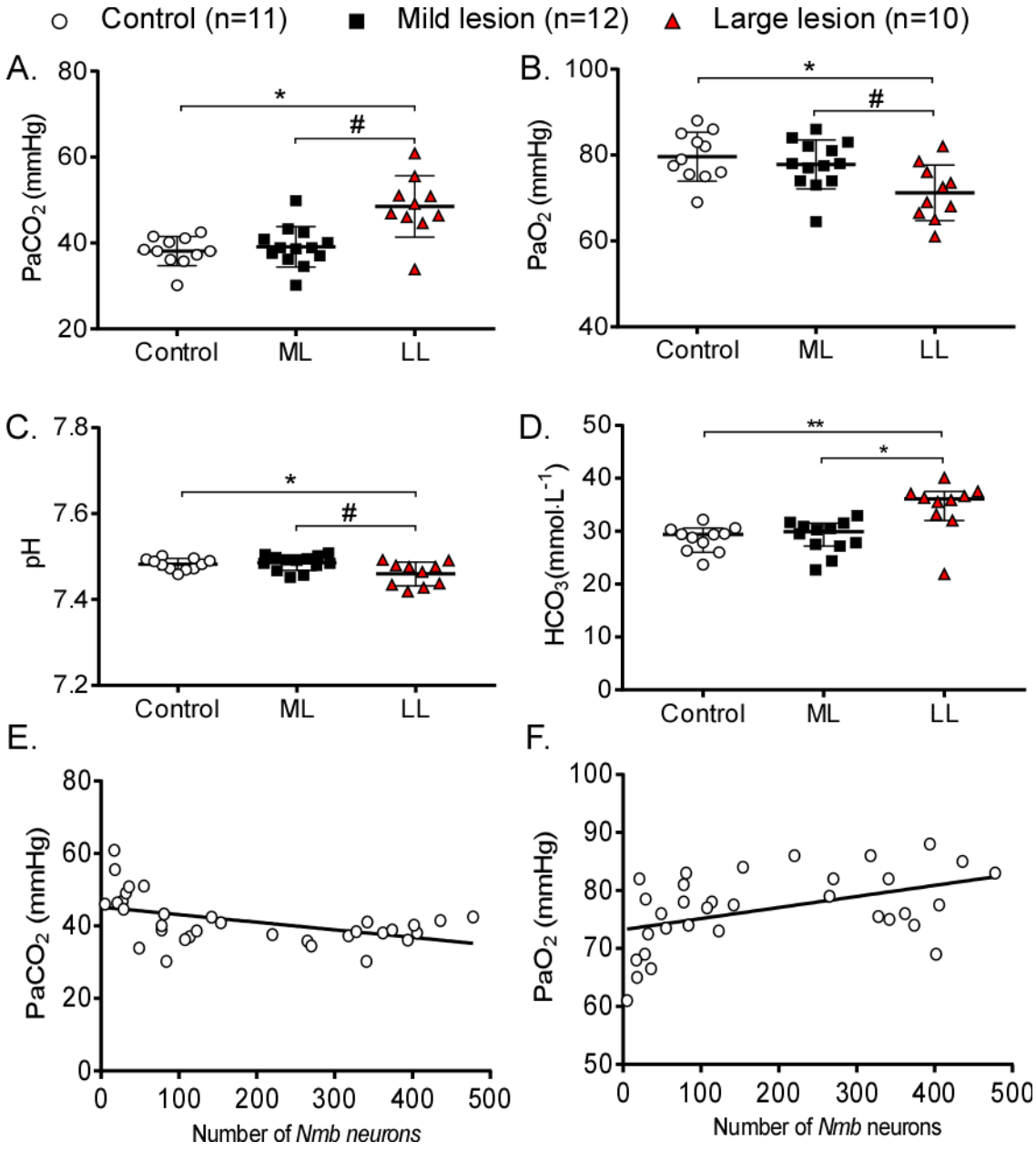

Accepted Article

This article is protected by copyright. All rights reserved.

Accepted Article

Figure 4: *Effect of RTN lesions on the breathing response to CO_2 under hyperoxia*

A. Experimental protocol. Down-pointing arrowheads indicate times when blood gases were measured (results in the next figure). Arrow pointing up indicate times when plethysmographic measurements were analyzed.

B. Representative plethysmographic recordings from a control rat, a rat with mild lesion and a rat with large lesion of RTN.

C. Effect of hypercapnia on f_R analyzed by 2-way RM ANOVA. f_R was significantly related to both inhaled gas mixture [F (4, 120) = 214.9; P<0.0001] and RTN lesions [F (2,30) = 37.2; P<0.0001]. There was also a highly significant interaction between these two factors [F (8,120) = 27.2; P<0.0001]. Bonferroni's multiple comparisons test: * control *vs.* large lesion (P= 0.0361 at 21/0, P < 0.0001 for all other gas mixtures); # mild *vs.* large lesion (P=0.0002 at 65/3, P<0.0001 at 65/6 and 65/9); & control *vs.* mild lesion (P < 0.0001 at 65/6, P=0.0059 at 65/9).

D. Effect of hypercapnia on V_T. 2-way RM ANOVA. V_T was significantly related to both inhaled gas mixture [F (4,120) = 110.2; P<0.0001] and extent of the RTN lesion [F (2, 30) = 19; P<0.0001]. There was also a highly significant interaction between these two factors [F (8, 120) = 8; P<0.0001]. Bonferroni's multiple comparisons test: *, control *vs.* large lesion (P=0.0069 at 21/0, P=0.0011 at 65/0, P=0.0002 at 65/3 and P<0.0001 for all other gas mixtures); #, mild *vs.* large lesion (P=0.0064 at 21/0, P=0.0011 at 65/0, P=0.0013 at 65/3, P<0.0001 at 65/6 and 56/9).

This article is protected by copyright. All rights reserved.

E. Effect of hypercapnia on V_E. 2-way RM ANOVA. V_E was significantly related to both inhaled gas mixture [F (4, 120) = 259.4; P<0.0001] and extent of the RTN lesion [F (2, 30) = 36.5; P<0.0001]. There was also a highly significant interaction between these two factors [F (8, 120) = 31.4; P<0.0001]. Bonferroni's multiple comparisons test: *, control *vs.* large lesion (P=0.0476 at 65/0, P<0.0001 for all other gas mixtures); #, mild *vs.* large lesion (P=0.0001 at 65/3, P<0.0001 at 65/6 and 56/9).

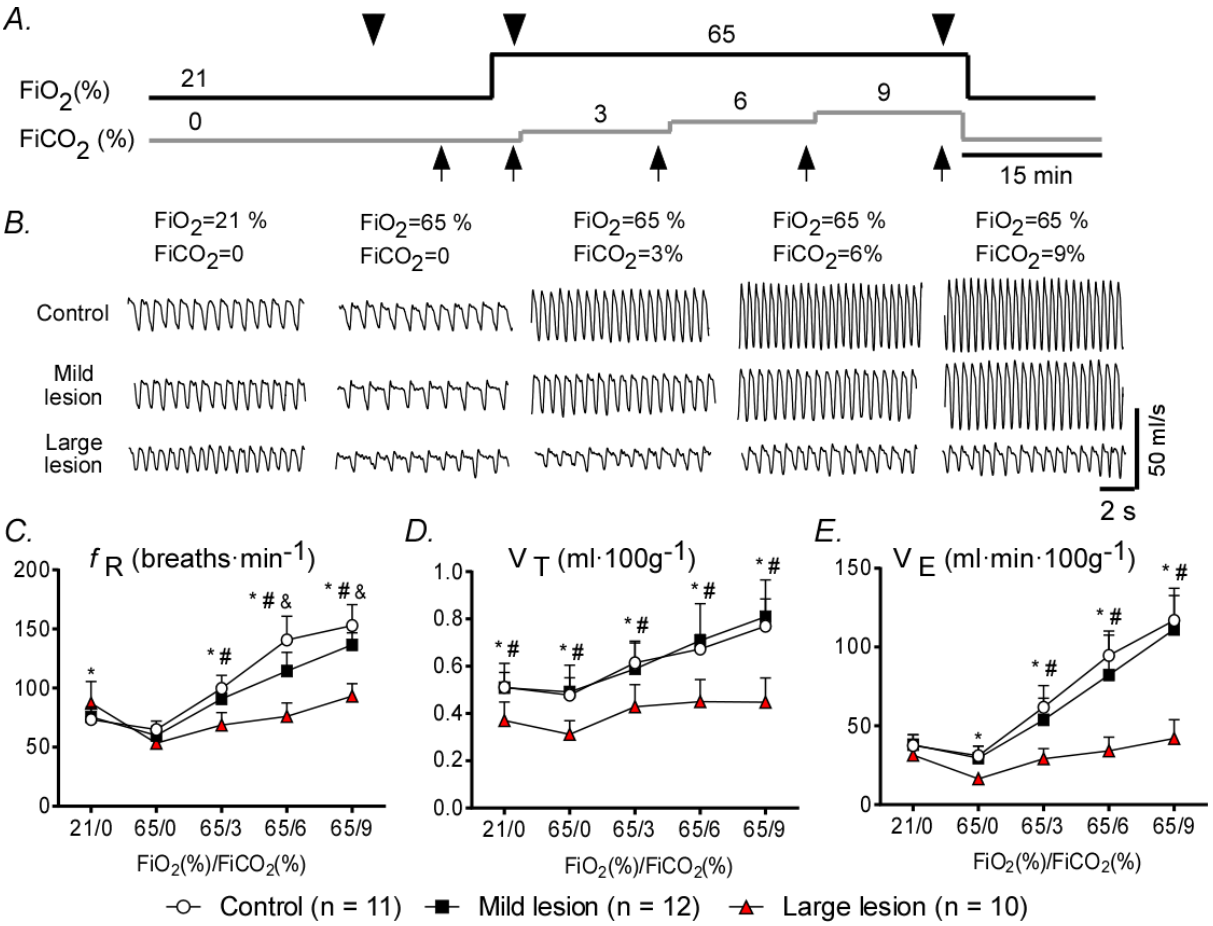

This article is protected by copyright. All rights reserved.

Accepted Article

Accepted Article

Figure 5: *Effect of RTN lesions on the hypercapnic ventilatory reflex*

This figure illustrates the differences between the breathing parameters recorded during exposure to 3, 6 and 9% $FiCO_2$ and the baseline values observed at the end of 2 minutes of hyperoxia (65/0 FiO_2/$FiCO_2$ time point in the preceding figure).

A. Effect of hyperoxic hypercapnia on Δf_R. Statistical analysis by 2-way RM ANOVA. Δf_R was significantly related to both $FiCO_2$ [F (2, 60) = 154.3; P<0.0001] and the extent of the RTN lesion [F (2, 30) = 36.7; P<0.0001]. There was also a highly significant interaction between these two factors [F (4, 60) = 10.2; P<0.0001]. Bonferroni's multiple comparisons: *, control *vs.* large lesion (P=0.004 at 3% $FiCO_2$, P < 0.0001 at 6% and 9% $FiCO_2$); &, control *vs.* mild lesion (P=0.0007), #, mild *vs.* large lesion (P=0.0235 at 3% $FiCO_2$, P<0.0001 at 6 and 9% $FiCO_2$).

B. Effect of hyperoxic hypercapnia on ΔV_T. Statistical analysis by 2-way RM ANOVA. ΔV_T was significantly related to both $FiCO_2$ [F (2, 60) = 53.1; P<0.0001] and extent of the RTN lesion [F (2, 30) = 3.6; P=0.0394]. There was also a highly significant interaction between these two factors [F (4, 60) = 11; P<0.0001]. Bonferroni's multiple comparisons: *, control *vs.* large lesion (P = 0.0003 at 9% $FiCO_2$); #, mild *vs.* large lesion (P<0.0001 at 9% $FiCO_2$).

C. Effect of hyperoxic hypercapnia on ΔV_E. Statistical analysis by 2-way RM ANOVA. ΔV_E was significantly related to $FiCO_2$ [F (2, 60) = 161.2; P<0.0001] and to the extent of the RTN lesion [F (2, 30) = 41.6; P<0.0001]. There was also a highly significant interaction between these two factors [F (4, 60) = 19.1; P<0.0001]. Bonferroni's multiple comparisons: *, control *vs.* large lesion (P=0.0089 at 3% $FiCO_2$, P<0.0001 at 6% and 9% $FiCO_2$); #, mild *vs.* large lesion (P<0.0001 at 6 and 9% $FiCO_2$).

This article is protected by copyright. All rights reserved.

D. Blood gases measured at two time points under hyperoxia (FiO_2=65%) indicated in Figure 4A. For both group of rats, first point was analyzed during 1-2 min of hyperoxia (FiO_2=65% and $FiCO_2$=0%) and the second point during hyperoxia hypercapnia (FiO_2=65% and $FiCO_2$=9%). 2-way RM ANOVA. There was a significant overall effect of hypercapnia on $PaCO_2$ [F (1, 13) = 141.1; P<0.0001] and of the RTN lesion [F (1, 13) = 29.3; P=0.0001]. However, there was no significant interaction between these two factors [F (1, 13) = 1.59; P=0.2295]. Bonferroni's multiple comparisons: *, control *vs.* large lesion for $PaCO_2$ levels (P=0.0019, at $FiCO_2$=0 and P<0.0001 at $FiCO_2$=9%). There was also an overall effect of hypercapnia on V_E [F (1, 13) = 187.7, P<0.0001] and of extent of the RTN lesion on V_E [F (1, 13) = 85.9; P<0.0001]. There was also an interaction between these two factors [F (1, 13) = 57.5; P<0.0001]. Bonferroni's multiple comparisons: # control *vs.* large lesion for V_E during high level of $PaCO_2$ (P<0.0001).

E. Relationship between ΔV_E and number of surviving RTN *Nmb* neurons at different $FiCO_2$. An inverse exponential function (represented) provided the best fit.

Accepted Article

This article is protected by copyright. All rights reserved.

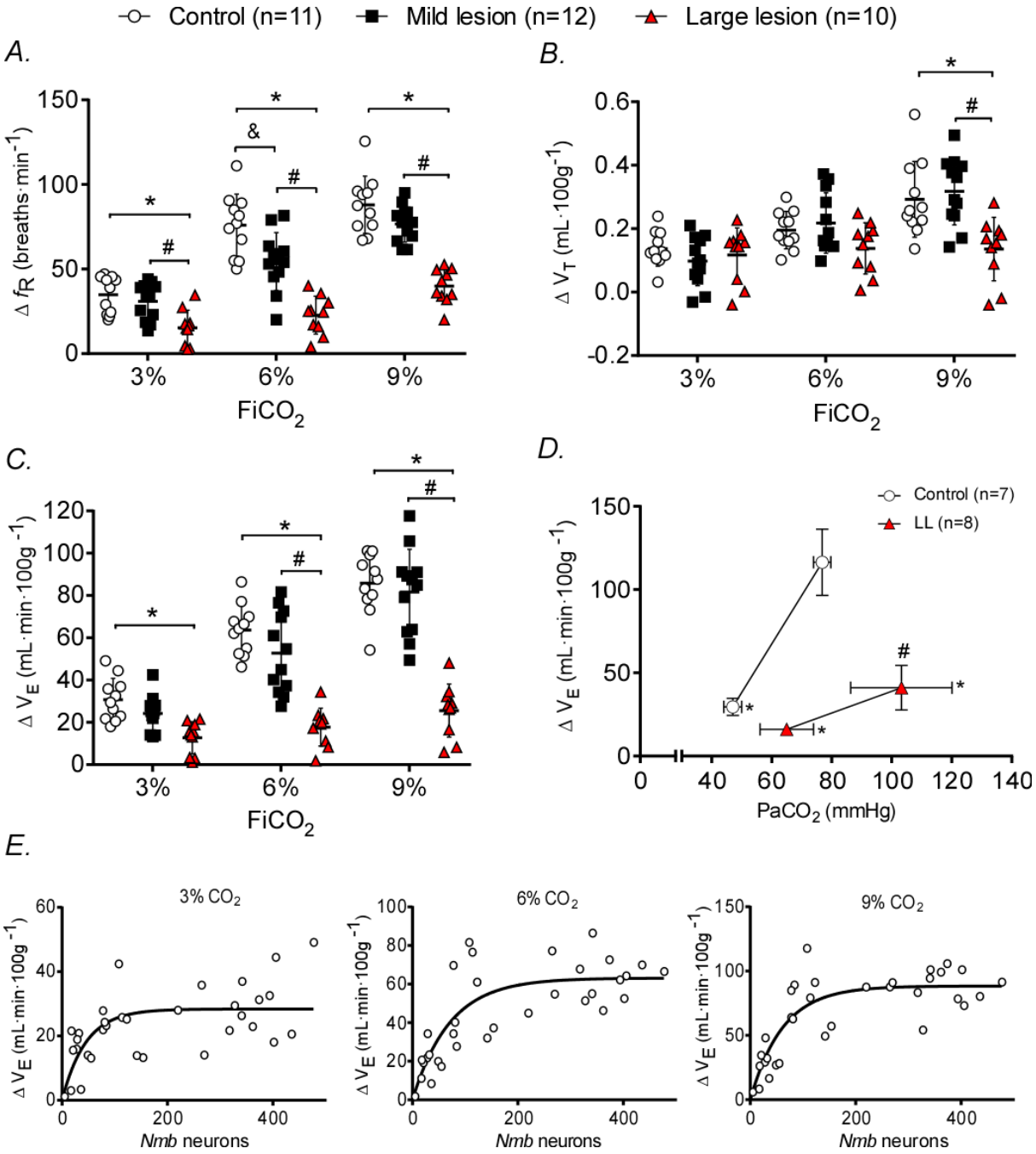

Accepted Article

This article is protected by copyright. All rights reserved.

Figure 6: *Effect of RTN lesions on arterial blood pressure (BP) and heart rate (HR) during hyperoxic hypercapnia or hypoxia.*

A. BP recorded under the various inhaled gas mixtures illustrated in Figure 4 A. 2-way RM ANOVA. There was a significant overall effect of the breathing mixture [F (4, 76) = 4.4; P =0.003] but no effect of lesion [F (2, 19) = 1.603; P=0.23] and no interaction between these two factors [F (8, 76) = 1.482; P=0.1779].

B. HR recorded under the same gas conditions as in panel A. 2-way RM ANOVA. There was a significant overall effect of the breathing mixture [F (4, 76) = 13.5; P<0.0001] but no effect of lesion [F (2, 19) = 1.3; P=0.2922] and no interaction between these two factors [F (8, 76) P=1.587; P=0.1428].

C. Effect of FiO_2 on BP. 2-way RM ANOVA. There was a significant overall effect of the breathing mixture [F (3, 51) = 8.5; P =0.0001] and the extent of the RTN lesion [F (2, 17) = 5.3; P = 0.0166] and a significant interaction between these two factors [F (6, 51) = 3.04; P=0.0128]. Bonferroni's multiple comparisons: Bonferroni's multiple comparisons: * control *vs.* large lesion (P =0.0035 at 12% FiO_2 or P=0.0002 at 10% FiO_2); # mild lesion *vs.* large lesion (P=0.0078).

D. Effect of FiO_2 on HR. 2-way RM ANOVA. There was a significant overall effect of the breathing mixture [F (3, 51) = 11.1; P < 0.0001] and extent of the RTN lesion [F (2, 17) = 4.4; P = 0.0282] and a significant interaction between these two factors [F (6, 51) = 3.5; P = 0.0053]. Bonferroni's multiple comparisons: *, control *vs.* large lesion (P=0.0002 at 15% FiO_2); &, control *vs.* mild (P=0.0208 at 15% FiO_2; P=0.048 at 12% FiO_2).

Accepted Article

This article is protected by copyright. All rights reserved.

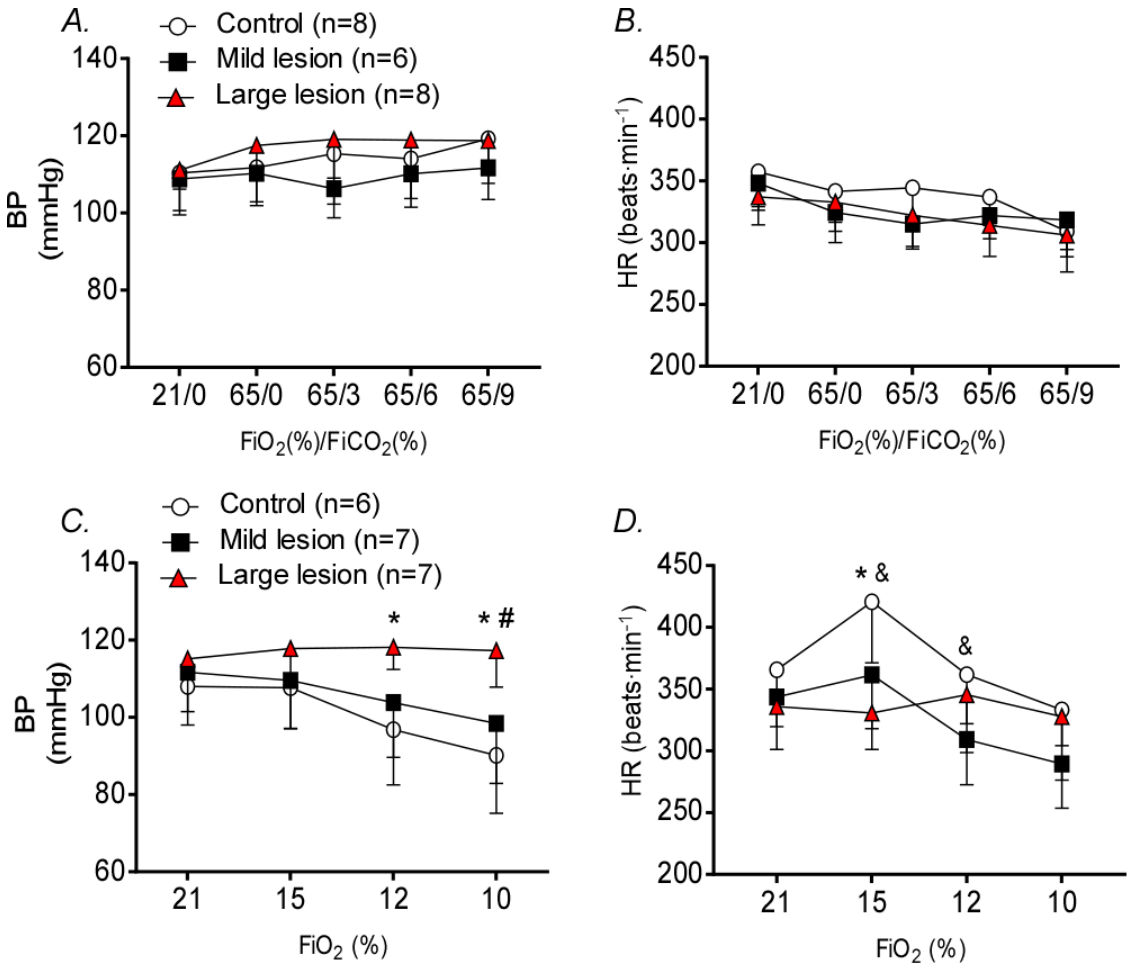

Accepted Article

This article is protected by copyright. All rights reserved.

Figure 7: *Hypoxic ventilatory reflex in rats with RTN lesions*

Accepted Article

A. Experimental protocol. Down-pointing arrowheads indicate times when blood gases were measured. Arrows pointing up indicate times when plethysmographic measurements were collected and analyzed.

B. Representative plethysmographic recordings from a control rat, a rat with mild lesion and a rat with large lesion of RTN.

C. Effect of hypoxia on Δf_R (f_R change relative to normoxia baseline). Statistical analysis by 2-way RM ANOVA. There was a significant overall effect of FiO_2 [F (2, 58) = 94.5; P<0.0001] and extent of the RTN lesion [F (2, 29) = 5.2; P=0.0117] and a highly significant interaction between these two factors [F (4, 58) = 4.97. P=0.0016]. Bonferroni's multiple comparisons: *, control *vs.* large lesion (P=0.003 at 12% FiO_2, P=0.0096 at 10% FiO_2); &, control *vs.* mild lesion (P=0.0044).

D. Effect of hypoxia on ΔV_T. Statistical analysis by 2-way RM ANOVA. There was no overall effect of FiO_2 [F (2, 58) = 2.9; P=0.0648] but there was a significant effect of RTN lesions [F (2, 29) = 12.6; P=0.0001] but significant interaction between these two factors [F (4, 58) = 4.7. P=0.0023]. Bonferroni's multiple comparisons: *, control *vs.* large lesion (P=0.0005 at 12% FiO_2, P < 0.0001 at 10% FiO_2); #, mild *vs.* large lesion (P=0.0022 at 12% FiO_2, P<0.0001 at 10% FiO_2).

E. Effect of hypoxia on ΔV_E. Statistical analysis by 2-way RM ANOVA. There was a significant overall effect of FiO_2 [F (2, 58) = 223; P<0.0001] but no effect of RTN lesions [F (2, 29) = 1.9; P =0.1673] and no interaction between these two factors [F (4, 58) = 1.8, P=0.1451].

This article is protected by copyright. All rights reserved.

F. Correlation between ΔV_E elicited by 10% FiO_2 and number of *Nmb* neurons. There was no significant correlation between the ΔV_E in response to hypoxia and the number of *Nmb* neurons (P=0.0627, Pearson r = -0.3328).

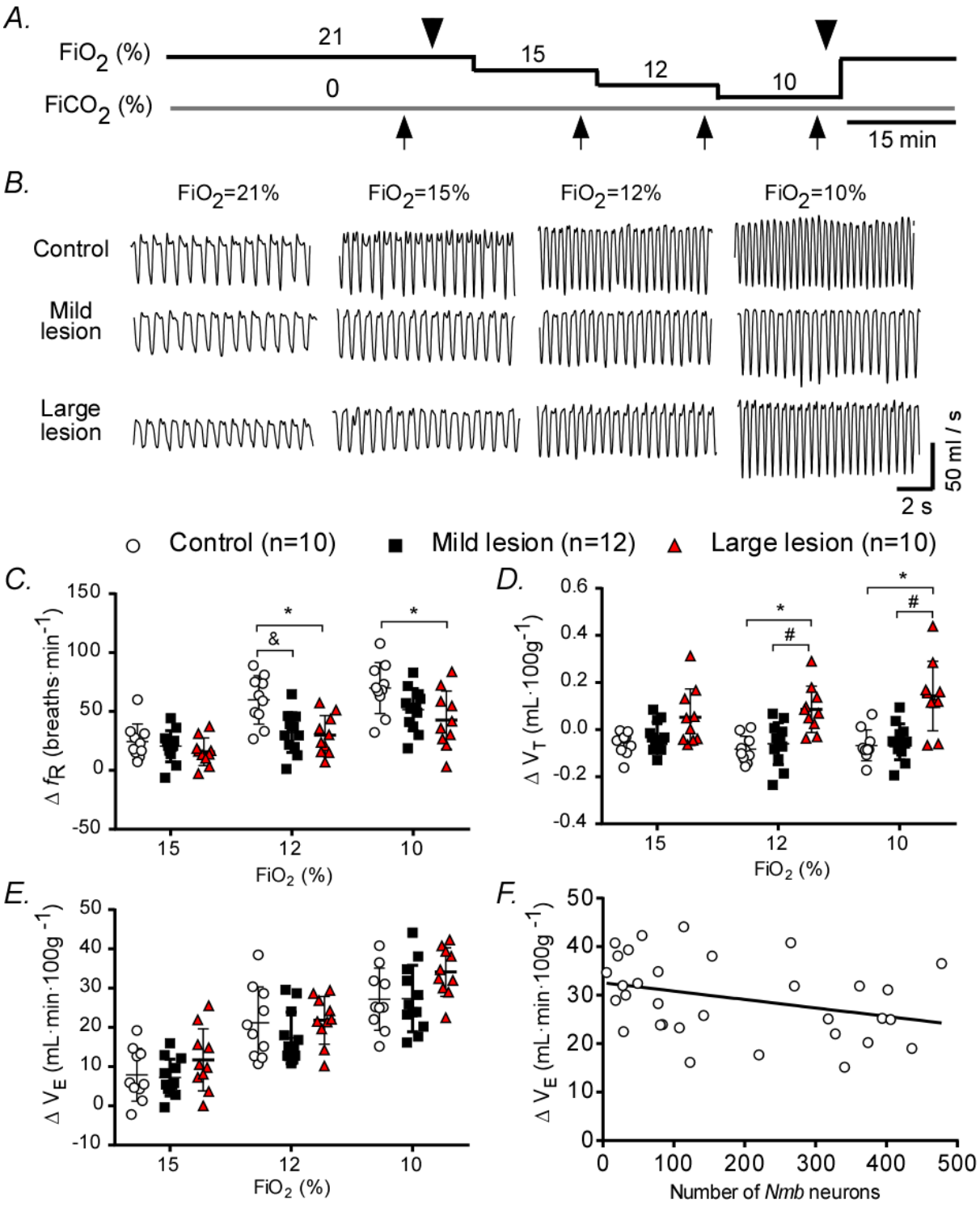

This article is protected by copyright. All rights reserved.

Accepted Article

Figure 8: *Effect of RTN lesions on sighing during normoxia or hypoxia*

A. Representative plethysmography recordings from a rat without RTN lesions (control), a rat with a moderate lesion and a rat with a large lesion of this nucleus. All recordings obtained under normoxia.

B. Higher resolution examples from the same rats illustrating that the kinetics of the sighs and their tidal volume (highlighted in red) were unaffected by lesions of the RTN.

C. Sigh frequency under normoxia (21% FiO_2) *vs.* hyperoxia (65% FiO_2). Statistics: 2-way RM ANOVA. Sigh frequency was significantly related to the O_2 level [$F(1, 32) = 48.5$; $P<0.0001$] and to the extent of RTN lesions [$F(2, 32) = 7.2$; $P=0.0026$] but there was no interaction between these two factors [$F(2, 32) = 0.06794$; $P=0.93$]. Bonferroni's multiple comparisons: *, control *vs.* large lesion ($P=0.006$ under normoxia, $P=0.01$ under hyperoxia)

D. Sigh frequency under three levels of hypoxia. 2-way RM ANOVA. Sigh frequency was significantly related to O_2 level [$F(2, 58) = 31.4$; $P<0001$] but there was no overall effect of RTN lesions [$F(2, 29) = 2.06$; $P=0.1456$] and no interaction between these two factors [$F(4, 58) = 1.58$; $P=0.1909$]. Bonferroni's multiple comparisons: #, control *vs.* mild lesion ($P=0.0374$ at 10% FiO_2).

Accepted Article

This article is protected by copyright. All rights reserved.

Accepted Article

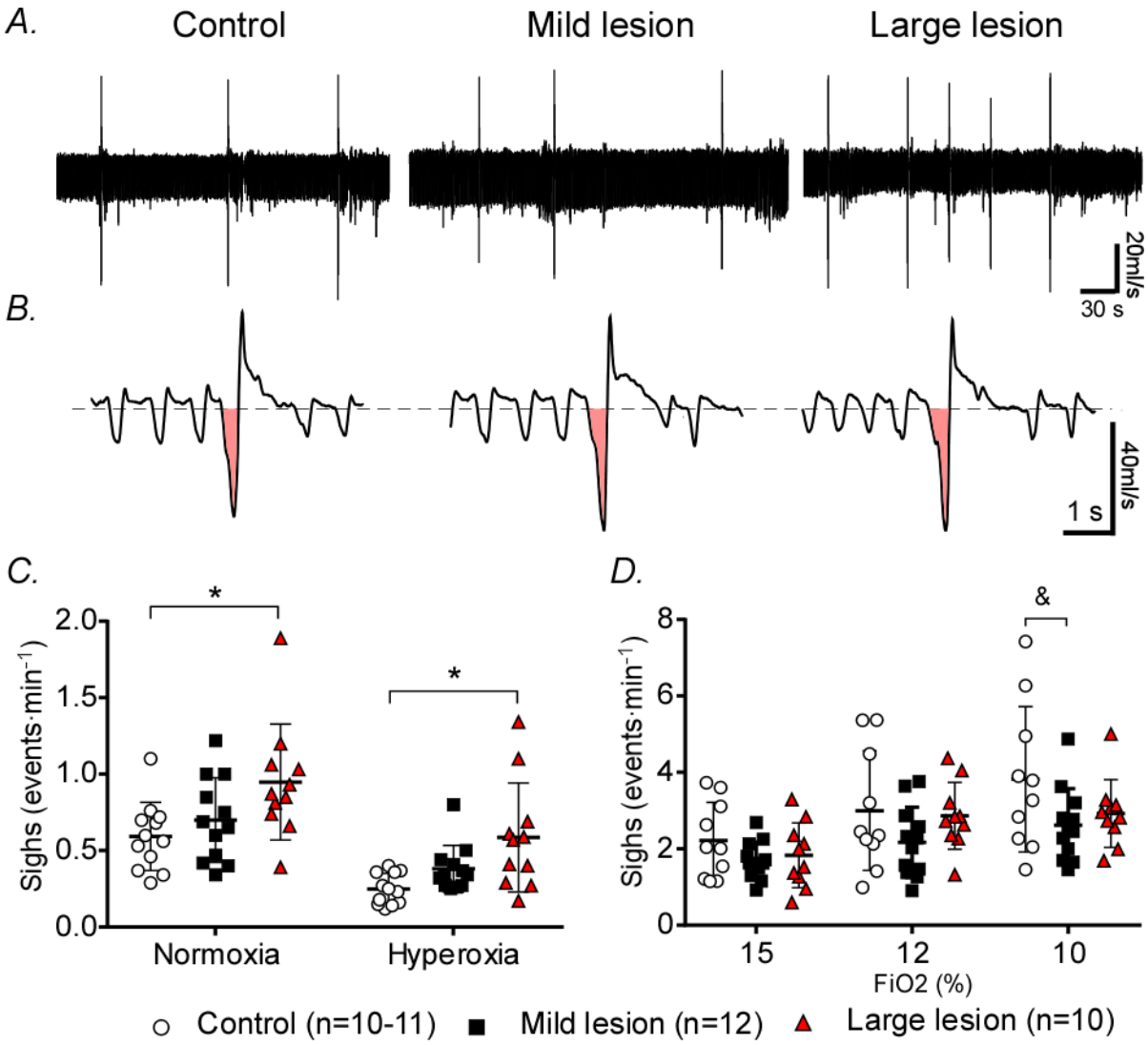

This article is protected by copyright. All rights reserved.

Figure 9: *Effect of RTN lesions on the ventilatory response to hyperoxia*

A. Experimental protocol. Down-pointing arrowheads indicate times when blood gases were measured (values not shown in figure). Arrow pointing up indicate times when plethysmographic measurements were analyzed.

B. Representative plethysmographic recordings from a control rat, a rat with a mild lesion and a rat with a large lesion of the RTN.

C. Effect of hyperoxia on f_R. Statistics: 2-way RM ANOVA. f_R was significantly related to FiO_2 [F (2, 62) = 45; P < 0.0001] but not the extent of the RTN lesion [F (2, 31) = 0.47; P=0.6396]. However, there was a highly significant interaction between these two factors [F (4, 62) = 15.4; P<0.0001]. Symbols represent statistical significance with Bonferroni's multiple comparisons test: * control *vs.* large lesion (P=0.0065 in normoxia; P=0.0015 after 1-3 min hyperoxia); # mild *vs.* large lesion (P=0.0035 at baseline; P=0.0138 after 1-3 min hyperoxia).

D. Effect of hyperoxia on V_T. Statistics: 2-way RM ANOVA. V_T was not correlated with to FiO_2 [F (2, 62) = 1.12; P=0.33] but was highly correlated with the extent of RTN lesions [F (2, 31) = 23.9; P<0.0001]. There was no interaction between these two factors [F (4, 62) = 0.99; P=0.4199]. Bonferroni's multiple comparisons test: * control *vs.* large lesion (P=0.003 in normoxia; P<0.0001 under hyperoxia at both time points); # mild *vs.* large lesion (P < 0.0001).

E. Effect of hyperoxia on V_E. Statistics: 2-way RM ANOVA. V_E was significantly related to both FiO_2 [F (2, 62) = 22.5; P<0.0001] and the extent of the RTN lesion [F (2, 31) = 19.5; P < 0.0001] and there was a highly significant interaction between these two factors [F (4,

This article is protected by copyright. All rights reserved.

Accepted Article

62) = 6.3; P=0.0002]. Bonferroni's multiple comparisons test: * control *vs.* large lesion (P<0.0001); # mild *vs.* large lesion (P=0.0071 at baseline; P<0.0001 under hyperoxia).

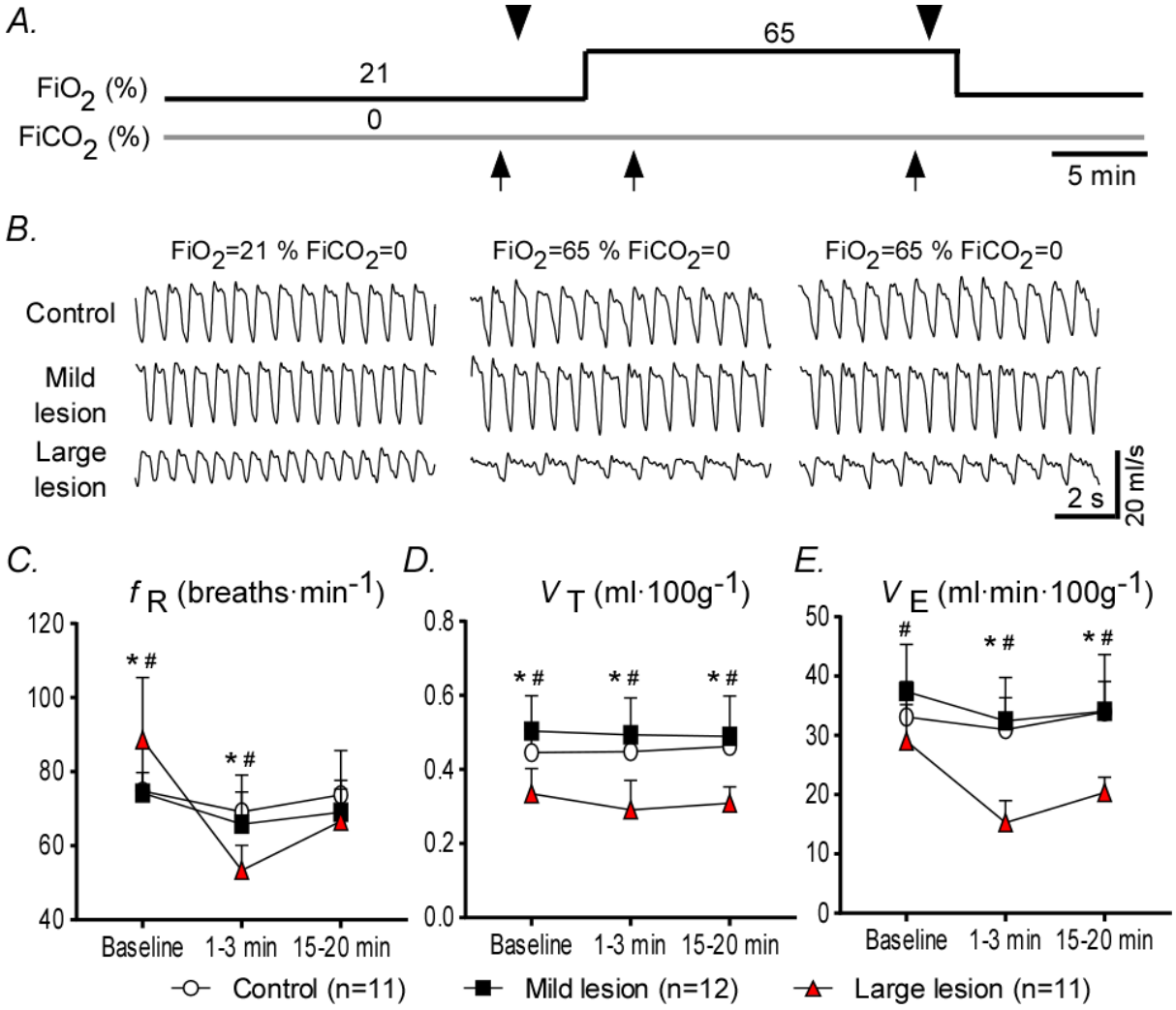

Accepted Article

This article is protected by copyright. All rights reserved.

Accepted Article

Figure 10: *Effect of RTN lesions on the ventilatory response to hyperoxia*

This figure illustrates the differences between the breathing parameters recorded early (1-3 min) after the start of hyperoxia or late (15-20 min) and the baseline values recorded in normoxia (see experimental design in preceding figure).

A. Effect of hyperoxia on Δf_R. Statistical analysis by 2-way RM ANOVA. Δf_R was significantly related to the duration of exposure to hyperoxia [F (1, 31) = 28.7; P<0.0001] and the extent of the RTN lesion [F (2, 31) = 19.4; P<0.0001]. There was also a highly significant interaction between these two factors [F (2, 31) = 5.7; P=0.0076]. Bonferroni's multiple comparisons test: * control *vs.* large lesion (P<0.0001 at 1-3 min, P=0.0001 at 15-20 min); #, mild *vs.* large lesions (P<0.0001 at 1-3 min, P=0.0017 at 15-20 min).

B. Effect of hyperoxic hypercapnia on ΔV_T. 2-way RM ANOVA. ΔV_T was related neither to hyperoxia [F (1, 31) = 0.64; P=0.4308] nor to the extent of the RTN lesion [F (2, 31) = 1.71; P=0.1970] and there was no significant interaction between these two factors [F (2, 31) = 0.3409; P=0.7137].

C. Effect of hyperoxic hypercapnia on ΔV_E. 2-way RM ANOVA. ΔV_E was significantly related to the time in hyperoxia [F (1, 31) = 9.8; P=0.0037] and to the extent of the RTN lesion [F (2, 31) = 11.6; P=0.0002]. There was no significant interaction between these two factors [F (2, 31) = 0.95; P=0.3973]. Bonferroni's multiple comparisons test: * control *vs.* large lesion (P < 0.0001 at 1-3 min, P=0.0014 at 15-20 min); #, mild *vs.* large lesions (P<0.0027 at 1-3 min).

D. $PaCO_2$ under normoxia and after 15-20 min of hyperoxia (time points indicated in Fig. 9A). 2-way RM ANOVA. There was a significant effect of FiO_2 [F (1, 19) = 111.6; P<0.0001] and of the extent of the RTN lesion [F (2, 19) = 27.76; P<0.0001] and a

This article is protected by copyright. All rights reserved.

significant interaction between these two factors [F (2, 19) = 23.19; P<0.0001]. Bonferroni's multiple comparisons test: * control *vs.* large lesion (P=0.0067 under normoxia, P<0.0001 under hyperoxia); #, mild *vs.* large lesions (P<0.0041 under normoxia, P<0.0001 under hyperoxia).

E. Relationship between ΔV_E and number of surviving RTN *Nmb* neurons after 1-3 min of hyperoxia modeled by linear regression. Significant positive correlation between the number of *Nmb* neurons and respiratory response to short hyperoxia (P=0.0001; Pearson r = 0.6156).

F. Relationship between ΔV_E and number of surviving RTN *Nmb* neurons during after 15-20 min of hyperoxia modeled by linear regression. Significant positive correlation between the number of *Nmb* neurons and respiratory response to short hyperoxia (P=0.0222; Pearson r = 0.3969).

Accepted Article

This article is protected by copyright. All rights reserved.

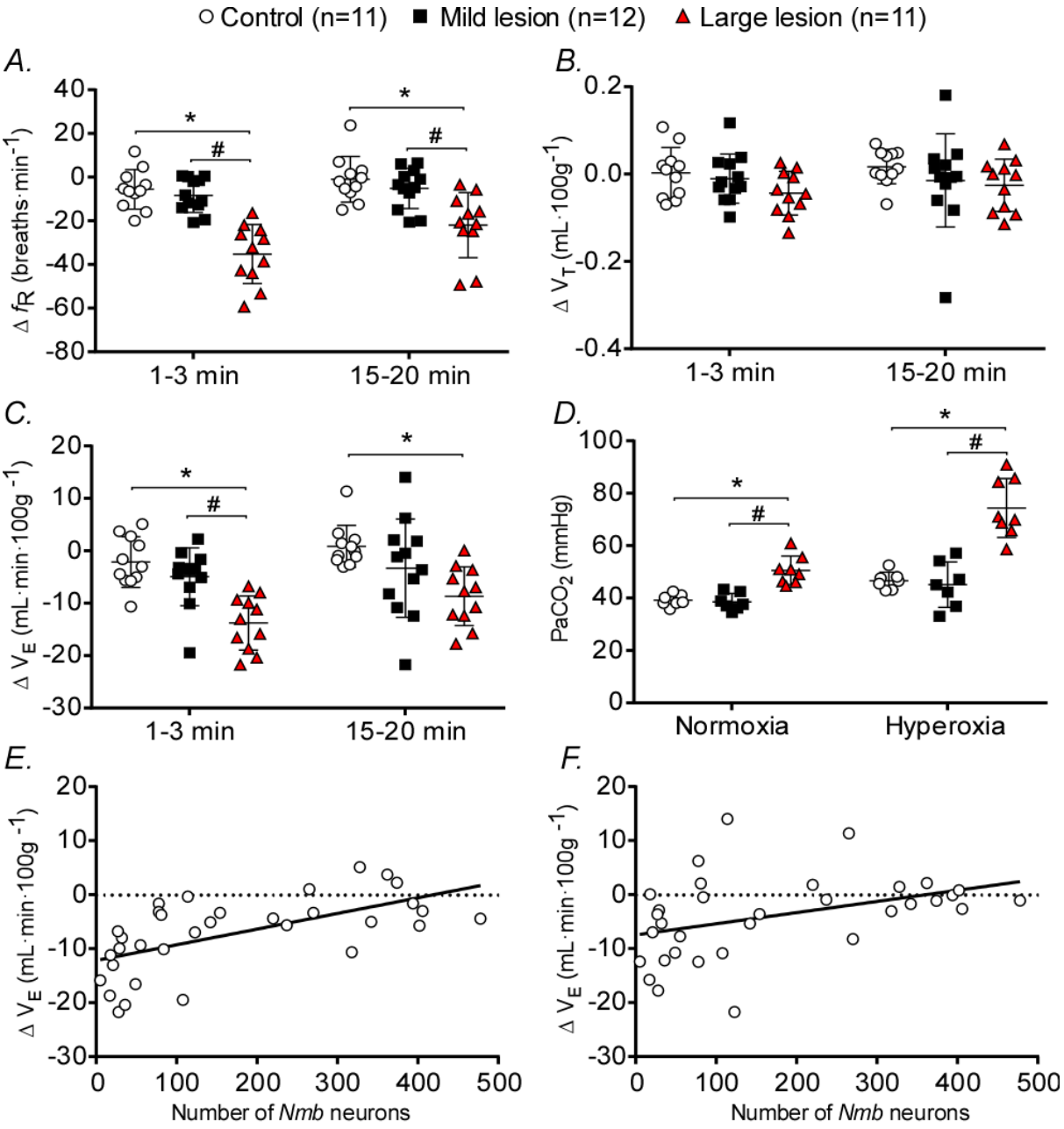

Accepted Article

This article is protected by copyright. All rights reserved.

Figure 11: *Breathing under normoxia: state-dependence and effect of RTN lesions*

A. Control rat. From top to bottom: EEG power spectrum (0–30 Hz), EEG (raw signal), neck EMG and air flow signal (plethysmography, inspiration downward). Excerpts were recorded during quiet waking, slow-wave sleep or REM sleep.

B. Rat with a large lesion of the RTN. Same data presentation.

C. Effect of RTN lesions on state-dependence of V_T. 2-way ANOVA. There was a significant overall effect of the state of vigilance [F (2, 83) = 24.8; P<0.0001] and of the extent of the RTN lesion [F (2, 83) = 25.0; P<0.0001] but no interaction between these two factors [F (4, 83) = 0.54; P=0.7051]. Bonferroni's multiple comparisons: *, control *vs.* large lesion (P=0.020 during wake; P=0.002 during SW-S; P=0.017 during REM sleep); #, mild *vs.* large lesion (P<0.0001 during wake and SW-S).

D. Effect of RTN lesions on state-dependence of f_R. 2-way ANOVA. There was a significant overall effect of the state of vigilance [F (2, 83) = 19.7; P<0.0001] and of the extent of the RTN lesion [F (2, 83) = 5.8; P=0.0043] on f_R but no interaction between these two factors [F (4, 83) = 0.79; P=0.53]. Bonferroni's multiple comparisons: #, mild *vs.* large lesion (P=0.0382).

E. Effect of RTN lesions on state-dependence of V_E. 2-way ANOVA. There was a significant overall effect of the state of vigilance [F (2, 83) = 6.3; P=0.0028] and of the extent of the RTN lesion on V_E [F (2, 83) = 13.4; P<0.0001] on V_E but no interaction between these two factors [F (4, 83) = 0.56; P=0.6935]. Bonferroni's multiple comparisons: *, control *vs.* large lesion (P=0.0339); #, mild *vs.* large lesion (P=0.0007 in the awake state; P=0.003 in SW-sleep).

This article is protected by copyright. All rights reserved.

Accepted Article

Accepted Article

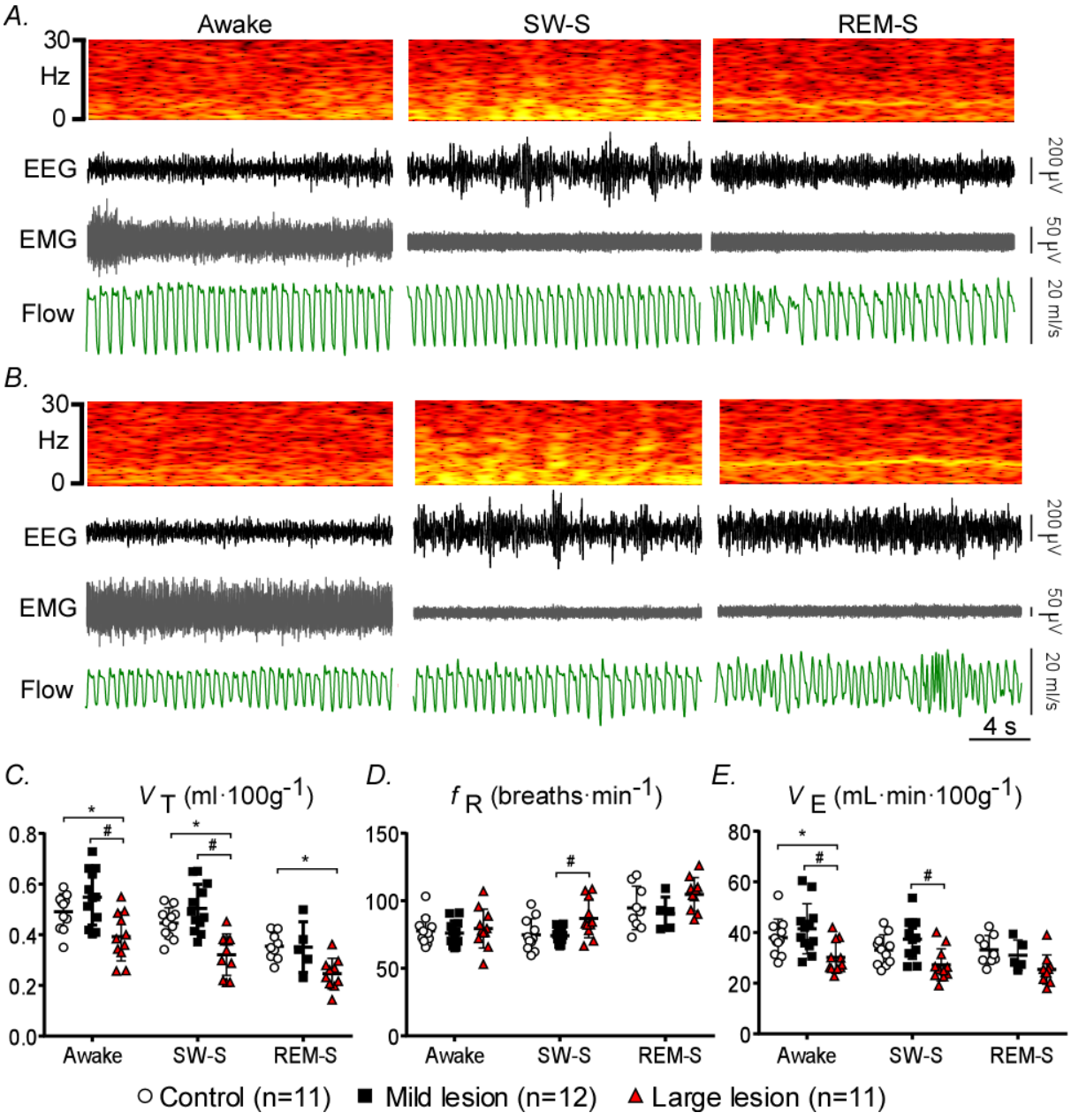

This article is protected by copyright. All rights reserved.

Figure 12: *Breathing under hyperoxia: state-dependence and effect of RTN lesions*

A. Effect of RTN lesions on state-dependency of V_T under hyperoxia. 2-way RM ANOVA. There was an overall effect of state of vigilance [F (1, 19) = 41.5; P<0.0001] and of the extent of the RTN lesions [F (1, 19) = 46; P<0.0001] but no significant interaction between both factors [F (1, 19) = 0.37; P=0.5520]. Bonferroni's multiple comparisons: *, control *vs.* large lesion (P<0.0001 for both stages of vigilance).

B. Effect of RTN lesions on state-dependency of f_R under hyperoxia. 2-way RM ANOVA. There was no overall effect of state of vigilance [F (1, 19) = 2.3; P=0.1456] but there was a significant effect of RTN lesions [F (1, 19) = 7.2; P=0.0148] but no significant interaction between both factors [F (1, 19) = 1; P=0.3305]. Bonferroni's multiple comparisons: *, control *vs.* large lesion (P=0.0139).

C. Effect of RTN lesions on state-dependency of V_E under hyperoxia. 2-way RM ANOVA. There was an overall effect of state of vigilance [(F (1, 19) = 35.7; P<0.0001] and the extent of the RTN lesion [F (1, 19) = 47.3; P<0.0001] but no significant interaction between both factors [F (1, 19) = 1.1; P=0.3068]. Bonferroni's multiple comparisons: *, control *vs.* large lesion (P<0.0001 for both stages of vigilance).

D. Effect of RTN lesions on breathing variability during the different sleep stages. 2-way ANOVA. There was an overall effect of sleep stage on the CV [F (2, 57) = 47.3; P<0.0001] but no significant effect of RTN lesions [F (1, 57) = 1.287; P=0.2614] and no interaction [F (2, 57) = 1.021; P=0.3668]. Bonferroni's multiple comparisons for control: * awake *vs.* REM (P=0.0003) and SW-S *vs*. REM (P<0.0001); and for large lesion: # awake *vs.* REM (P<0.0001) and SW-S *vs*. REM (P<0.0001).

This article is protected by copyright. All rights reserved.

Accepted Article

E. Effect of hyperoxia on breathing variability during awake and SW-S in rats with RTN lesions and control rats. 2-way RM ANOVA. There was an overall effect of hyperoxia [F (1, 19) = 9.659; P= 0.0058] and extent of the RTN lesion [F (1, 19) = 9.866; P=0.0054], however no interaction between these two factors [F (1, 19) = 1.893; P=0.1849]. Bonferroni's multiple comparisons: * Control *vs.* Large lesion (P=0.0030).

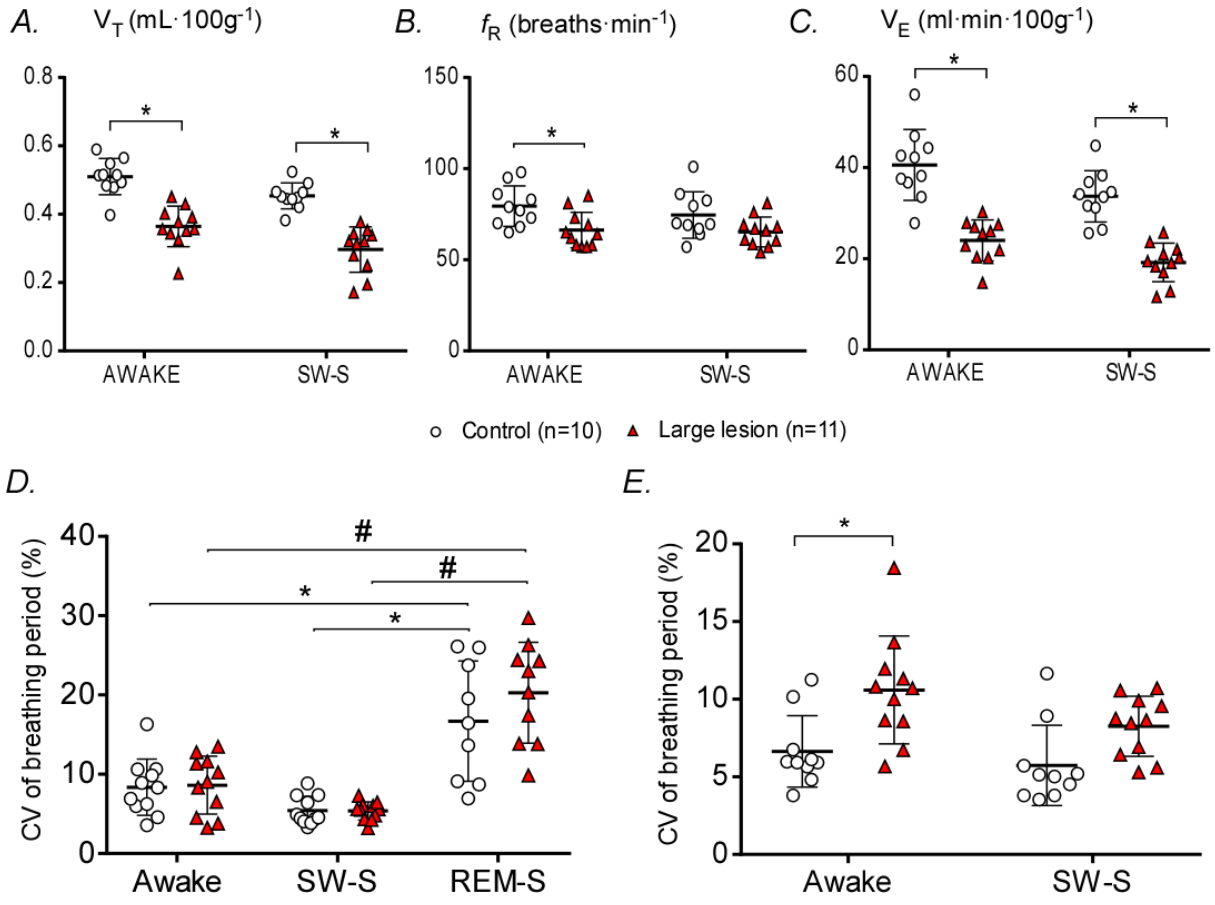

This article is protected by copyright. All rights reserved.

REFERENCES

Accepted Article

Abbott SB, Stornetta RL, Coates MB & Guyenet PG. (2011). Phox2b-expressing neurons of the parafacial region regulate breathing rate, inspiration, and expiration in conscious rats. *J Neurosci* **31,** 16410-16422.

Aicher SA, Saravay RH, Cravo S, Jeske I, Morrison SF, Reis DJ & Milner TA. (1996). Monosynaptic projections from the nucleus tractus solitarii to C1 adrenergic neurons in the rostral ventrolateral medulla: Comparison with input from the caudal ventrolateral medulla. *J Comp Neurology* **373,** 62-75.

Amiel J, Dubreuil V, Ramanantsoa N, Fortin G, Gallego J, Brunet JF & Goridis C. (2009). PHOX2B in respiratory control: lessons from congenital central hypoventilation syndrome and its mouse models. *Respir Physiol Neurobiol* **168,** 125-132.

Amiel J, Laudier B, Attie-Bitach T, Trang H, de PL, Gener B, Trochet D, Etchevers H, Ray P, Simonneau M, Vekemans M, Munnich A, Gaultier C & Lyonnet S. (2003). Polyalanine expansion and frameshift mutations of the paired-like homeobox gene PHOX2B in congenital central hypoventilation syndrome. *Nat Genet* **33,** 459-461.

Basting TM, Burke PG, Kanbar R, Viar KE, Stornetta DS, Stornetta RL & Guyenet PG. (2015). Hypoxia Silences Retrotrapezoid Nucleus Respiratory Chemoreceptors via Alkalosis. *J Neurosci* **35,** 527-543.

Bell HJ, Ferguson C, Kehoe V & Haouzi P. (2009). Hypocapnia increases the prevalence of hypoxia-induced augmented breaths. *Am J Physiol Regul Integr Comp Physiol* **296,** R334-R344.

This article is protected by copyright. All rights reserved.

Brust RD, Corcoran AE, Richerson GB, Nattie E & Dymecki SM. (2014). Functional and developmental identification of a molecular subtype of brain serotonergic neuron specialized to regulate breathing dynamics. *Cell reports* **9,** 2152-2165.

Burke PG, Abbott SB, Coates MB, Viar KE, Stornetta RL & Guyenet PG. (2014). Optogenetic stimulation of adrenergic C1 neurons causes sleep state-dependent cardiorespiratory stimulation and arousal with sighs in rats. *Am J Respir Crit Care Med* **190,** 1301-1310.

Burke PG, Kanbar R, Basting TM, Hodges WM, Viar KE, Stornetta RL & Guyenet PG. (2015a). State-dependent control of breathing by the retrotrapezoid nucleus. *J Physiol* **593,** 2909-2926.

Burke PG, Kanbar R, Viar KE, Stornetta RL & Guyenet PG. (2015b). Selective optogenetic stimulation of the retrotrapezoid nucleus in sleeping rats activates breathing without changing blood pressure or causing arousal or sighs. *J Appl Physiol (1985)* **118,** 1491-1501.

Carroll MS, Patwari PP, Kenny AS, Brogadir CD, Stewart TM & Weese-Mayer DE. (2014). Residual chemosensitivity to ventilatory challenges in genotyped congenital central hypoventilation syndrome. *J Appl Physiol (1985)* **116,** 439-450.

Conrad SC, Nichols NL, Ritucci NA, Dean JB & Putnam RW. (2009). Development of chemosensitivity in neurons from the nucleus tractus solitarii (NTS) of neonatal rats. *Respir Physiol Neurobiol* **166,** 4-12.

Coote JH. (1982). Respiratory and circulatory control during sleep. *J Exp Bio* **100,** 223-244.

Accepted Article

This article is protected by copyright. All rights reserved.

Dauger S, Pattyn A, Lofaso F, Gaultier C, Goridis C, Gallego J & Brunet JF. (2003). Phox2b controls the development of peripheral chemoreceptors and afferent visceral pathways. *Development* **130,** 6635-6642.

Dejours P. (1962). Chemoreflexes in breathing. *Physiol Rev* **42,** 335-358.

Dempsey B, Le S, Turner A, Bokiniec P, Ramadas R, Bjaalie JG, Menuet C, Neve R, Allen AM, Goodchild AK & McMullan S. (2017). Mapping and Analysis of the Connectome of Sympathetic Premotor Neurons in the Rostral Ventrolateral Medulla of the Rat Using a Volumetric Brain Atlas. *Front Neural Circuits* **11,** 9.

Dong L, Krewson EA & Yang LV. (2017). Acidosis Activates Endoplasmic Reticulum Stress Pathways through GPR4 in Human Vascular Endothelial Cells. *Int J Mol Sci* **18**.

Dubreuil V, Ramanantsoa N, Trochet D, Vaubourg V, Amiel J, Gallego J, Brunet JF & Goridis C. (2008). A human mutation in Phox2b causes lack of CO2 chemosensitivity, fatal central apnoea and specific loss of parafacial neurons. *Proc Natl Acad Sci USA* **105,** 1067-1072.

Gargaglioni LH, Hartzler LK & Putnam RW. (2010). The locus coeruleus and central chemosensitivity. *Respir Physiol Neurobiol* **173,** 264-273.

Gestreau C, Heitzmann D, Thomas J, Dubreuil V, Bandulik S, Reichold M, Bendahhou S, Pierson P, Sterner C, Peyronnet-Roux J, Benfriha C, Tegtmeier I, Ehnes H, Georgieff M, Lesage F, Brunet JF, Goridis C, Warth R & Barhanin J. (2010). Task2 potassium channels set central respiratory CO2 and O2 sensitivity. *Proc Natl Acad Sci USA* **107,** 2325-2330.

Accepted Article

This article is protected by copyright. All rights reserved.

Goridis C, Dubreuil V, Thoby-Brisson M, Fortin G & Brunet JF. (2010). Phox2b, congenital central hypoventilation syndrome and the control of respiration. *Semin Cell Dev Biol* **21,** 814-822.

Gourine AV & Kasparov S. (2011). Astrocytes as brain interoceptors. *Exp Physiol* **96,** 411-416.

Grundy D. (2015). Principles and standards for reporting animal experiments in The Journal of Physiology and Experimental Physiology. *J Physiol* **593,** 2547-2549.

Guyenet PG, Bayliss DA, Stornetta RL, Kanbar R, Shi Y, Holloway BB, Souza G, Basting TM, Abbott SBG & Wenker IC. (2017). Interdependent feedback regulation of breathing by the carotid bodies and the retrotrapezoid nucleus. *J Physiol* (in print).

Guyenet PG, Bayliss DA, Stornetta RL, Ludwig MG, Kumar NN, Shi Y, Burke PG, Kanbar R, Basting TM, Holloway BB & Wenker IC. (2016). Proton detection and breathing regulation by the retrotrapezoid nucleus. *J Physiol* **594,** 1529-1551.

Hawryluk JM, Moreira TS, Takakura AC, Wenker IC, Tzingounis AV & Mulkey DK. (2012). KCNQ channels determine serotonergic modulation of ventral surface chemoreceptors and respiratory drive. *J Neurosci* **32,** 16943-16952.

Hennessy ML, Corcoran AE, Brust RD, Chang Y, Nattie EE & Dymecki SM. (2017). Activity of Tachykinin1-Expressing Pet1 Raphe Neurons Modulates the Respiratory Chemoreflex. *J Neurosci* **37,** 1807-1819.

Hodges MR, Tattersall GJ, Harris MB, McEvoy SD, Richerson DN, Deneris ES, Johnson RL, Chen ZF & Richerson GB. (2008). Defects in breathing and thermoregulation in mice with near-complete absence of central serotonin neurons. *J Neurosci* **28,** 2495-2505.

Accepted Article

This article is protected by copyright. All rights reserved.

Huckstepp RT, Cardoza KP, Henderson LE & Feldman JL. (2015). Role of parafacial nuclei in control of breathing in adult rats. *J Neurosci* **35,** 1052-1067.

Huckstepp RT, Henderson LE, Cardoza KP & Feldman JL. (2016). Interactions between respiratory oscillators in adult rats. *eLife* **5,** e14203.

Koshiya N, Huangfu D & Guyenet PG. (1993). Ventrolateral medulla and sympathetic chemoreflex in the rat. *Brain Res* **609,** 174-184.

Kumar NN, Velic A, Soliz J, Shi Y, Li K, Wang S, Weaver JL, Sen J, Abbott SB, Lazarenko RM, Ludwig MG, Perez-Reyes E, Mohebbi N, Bettoni C, Gassmann M, Suply T, Seuwen K, Guyenet PG, Wagner CA & Bayliss DA. (2015). Regulation of breathing by CO_2 requires the proton-activated receptor GPR4 in retrotrapezoid nucleus neurons. *Science* **348,** 1255-1260.

Kumar P & Prabhakar NR. (2012). Peripheral chemoreceptors: function and plasticity of the carotid body. *Compr Physiol* **2,** 141-219.

Kuo FS, Falquetto B, Chen D, Oliveira LM, Takakura AC & Mulkey DK. (2016). In vitro characterization of noradrenergic modulation of chemosensitive neurons in the retrotrapezoid nucleus. *J Neurophysiol* **116,** 1024-1035.

Lazarenko RM, Stornetta RL, Bayliss DA & Guyenet PG. (2011). Orexin A activates retrotrapezoid neurons in mice. *Respir Physiol Neurobiol* **175,** 283-287.

Li A & Nattie E. (2010). Antagonism of rat orexin receptors by almorexant attenuates central chemoreception in wakefulness in the active period of the diurnal cycle. *J Physiol* **588,** 2935-2944.

This article is protected by copyright. All rights reserved.

Accepted Article

Li P, Janczewski WA, Yackle K, Kam K, Pagliardini S, Krasnow MA & Feldman JL. (2016). The peptidergic control circuit for sighing. *Nature* **530,** 293-297.

Mahadevan MS, Baird S, Bailly JE, Shutler GG, Sabourin LA, Tsilfidis C, Neville CE, Narang M & Korneluk RG. (1995). Isolation of a novel G protein-coupled receptor (GPR4) localized to chromosome 19q13.3. *Genomics* **30,** 84-88.

Malheiros-Lima MR, Totola LT, Takakura AC & Moreira TS. (2018). Impaired chemosensory control of breathing after depletion of bulbospinal catecholaminergic neurons in rats. *Pflugers Archiv* **470**:277-293.

Marina N, Abdala AP, Trapp S, Li A, Nattie EE, Hewinson J, Smith JC, Paton JF & Gourine AV. (2010). Essential role of Phox2b-expressing ventrolateral brainstem neurons in the chemosensory control of inspiration and expiration. *J Neurosci* **30,** 12466-12473.

Moreira TS, Takakura AC, Colombari E & Guyenet PG. (2006). Central chemoreceptors and sympathetic vasomotor outflow. *J Physiol* **577,** 369-386.

Mouradian GC, Forster HV & Hodges MR. (2012). Acute and chronic effects of carotid body denervation on ventilation and chemoreflexes in three rat strains. *J Physiol* **590,** 3335-3347.

Mulkey DK, Rosin DL, West G, Takakura AC, Moreira TS, Bayliss DA & Guyenet PG. (2007). Serotonergic neurons activate chemosensitive retrotrapezoid nucleus neurons by a pH-independent mechanism. *J Neurosci* **27,** 14128-14138.

Mulkey DK, Stornetta RL, Weston MC, Simmons JR, Parker A, Bayliss DA & Guyenet PG. (2004). Respiratory control by ventral surface chemoreceptor neurons in rats. *Nat Neurosci* **7,** 1360-1369.

This article is protected by copyright. All rights reserved.

Accepted Article

Accepted Article

Nattie EE & Li A. (2002a). Substance P-saporin lesion of neurons with NK1 receptors in one chemoreceptor site in rats decreases ventilation and chemosensitivity. *J Physiol* **544,** 603-616.

Nattie EE & Li A. (2002b). Substance P-saporin lesion of neurons with NK1 receptors in one chemoreceptor site in rats decreases ventilation and chemosensitivity. *J Physiol* **544,** 603-616.

Nattie EE, Li, A. (2012). Central Chemoreceptors: Locations and Functions. *Comp Physiol* **2,** 221-254.

Nobuta H, Cilio MR, Danhaive O, Tsai HH, Tupal S, Chang SM, Murnen A, Kreitzer F, Bravo V, Czeisler C, Gokozan HN, Gygli P, Bush S, Weese-Mayer DE, Conklin B, Yee SP, Huang EJ, Gray PA, Rowitch D & Otero JJ. (2015). Dysregulation of locus coeruleus development in congenital central hypoventilation syndrome. *Acta Neuropathol* **130,** 171-183.

Oliveira LM, Moreira TS, Kuo FS, Mulkey DK & Takakura AC. (2016). alpha1- and alpha2-adrenergic receptors in the retrotrapezoid nucleus differentially regulate breathing in anesthetized adult rats. *J Neurophysiol* **116,** 1036-1048.

Pepper DR, Landauer RC & Kumar P. (1995). Postnatal development of CO_2-O_2 interaction in the rat carotid body in vitro. *J Physiol* **485** (Pt 2)**,** 531-541.

Perez IA & Keens TG. (2013). Peripheral chemoreceptors in congenital central hypoventilation syndrome. *Respir Physiol Neurobiol* **185,** 186-193.

This article is protected by copyright. All rights reserved.

Ptak K, Yamanishi T, Aungst J, Milescu LS, Zhang R, Richerson GB & Smith JC. (2009). Raphe neurons stimulate respiratory circuit activity by multiple mechanisms via endogenously released serotonin and substance P. *J Neurosci* **29,** 3720-3737.

Ramanantsoa N, Hirsch MR, Thoby-Brisson M, Dubreuil V, Bouvier J, Ruffault PL, Matrot B, Fortin G, Brunet JF, Gallego J & Goridis C. (2011). Breathing without CO2 chemosensitivity in conditional Phox2b mutants. *J Neurosci* **31,** 12880-12888.

Ramirez JM. (2014). The integrative role of the sigh in psychology, physiology, pathology, and neurobiology. *Prog brain res* **209,** 91-129.

Ray RS, Corcoran AE, Brust RD, Kim JC, Richerson GB, Nattie E & Dymecki SM. (2011). Impaired respiratory and body temperature control upon acute serotonergic neuron inhibition. *Science* **333,** 637-642.

Reyes R, Duprat F, Lesage F, Fink M, Salinas M, Farman N & Lazdunski M. (1998). Cloning and expression of a novel pH-sensitive two pore domain K+ channel from human kidney. *J Biol Chem* **273,** 30863-30869.

Rodman JR, Curran AK, Henderson KS, Dempsey JA & Smith CA. (2001). Carotid body denervation in dogs: eupnea and the ventilatory response to hyperoxic hypercapnia. *J Appl Physiol (1985)* **91,** 328-335.

Ruffault PL, D'Autreaux F, Hayes JA, Nomaksteinsky M, Autran S, Fujiyama T, Hoshino M, Hagglund M, Kiehn O, Brunet JF, Fortin G & Goridis C. (2015). The retrotrapezoid nucleus neurons expressing Phox2b and Atoh-1 are essential for the respiratory response to CO2. *eLife* **4,** doi: 10.7554/eLife.07051.

Shi Y, Abe C, Holloway BB, Shu S, Kumar NN, Weaver JL, Sen J, Perez-Reyes E, Stornetta RL, Guyenet PG & Bayliss DA. (2016). Nalcn Is a "Leak" Sodium Channel That

This article is protected by copyright. All rights reserved.

Accepted Article

Regulates Excitability of Brainstem Chemosensory Neurons and Breathing. *J Neurosci* **36,** 8174-8187.

Shi Y, Stornetta RL, Stornetta DS, Onengut-Gumuscu S, Farber EA, Turner SD, Guyenet PG & Bayliss DA. (2017). Neuromedin B Expression Defines the Mouse Retrotrapezoid Nucleus. *J Neurosci* **37,** 11744-11757.

Smith CA, Rodman JR, Chenuel BJ, Henderson KS & Dempsey JA. (2006). Response time and sensitivity of the ventilatory response to CO2 in unanesthetized intact dogs: central vs. peripheral chemoreceptors. *J Appl Physiol (1985)* **100,** 13-19.

Solomon IC, Edelman NH & O'Neill MH. (2000). CO_2/H^+ chemoreception in the cat pre-Botzinger complex in vivo. *J Appl Physiol (1985)* **88,** 1996-2007.

Stornetta RL, Moreira TS, Takakura AC, Kang BJ, Chang DA, West GH, Brunet JF, Mulkey DK, Bayliss DA & Guyenet PG. (2006). Expression of Phox2b by brainstem neurons involved in chemosensory integration in the adult rat. *J Neurosci* **26,** 10305-10314.

Sun MK & Reis DJ. (1993). Differential responses of barosensitive neurons of rostral ventrolateral medulla to hypoxia in rats. *Brain Res* **609,** 333-337.

Sun MK & Reis DJ. (1994). Hypoxia selectively excites vasomotor neurons of rostral ventrolateral medulla in rats. *Am J Physiol Regul Integr Comp Physiol* **266,** R245-R256.

Takakura AC, Barna BF, Cruz JC, Colombari E & Moreira TS. (2014). Phox2b-expressing retrotrapezoid neurons and the integration of central and peripheral chemosensory control of breathing in conscious rats. *Exp Physiol* **99,** 571-585.

Accepted Article

This article is protected by copyright. All rights reserved.

Takakura AC, Moreira TS, Colombari E, West GH, Stornetta RL & Guyenet PG. (2006). Peripheral chemoreceptor inputs to retrotrapezoid nucleus (RTN) CO_2-sensitive neurons in rats. *J Physiol* **572,** 503-523.

Takakura AC, Moreira TS, Stornetta RL, West GH, Gwilt JM & Guyenet PG. (2008). Selective lesion of retrotrapezoid *Phox2b*-expressing neurons raises the apnoeic threshold in rats. *J Physiol* **586,** 2975-2991.

Tan W, Pagliardini S, Yang P, Janczewski WA & Feldman JL. (2010). Projections of preBotzinger complex neurons in adult rats. *J Comp Neurol* **518,** 1862-1878.

Teran FA, Massey CA & Richerson GB. (2014). Serotonin neurons and central respiratory chemoreception: where are we now? *Prog Brain Res* **209,** 207-233.

Viemari JC & Ramirez JM. (2006). Norepinephrine Differentially Modulates Different Types of Respiratory Pacemaker and Nonpacemaker Neurons. *J Neurophysiol* **95,** 2070-2082.

Weese-Mayer DE, Berry-Kravis EM, Ceccherini I, Keens TG, Loghmanee DA & Trang H. (2010). An official ATS clinical policy statement: Congenital central hypoventilation syndrome: genetic basis, diagnosis, and management. *Am J Respir Crit Care Med* **181,** 626-644.

Wenker IC, Abe C, Viar KE, Stornetta DS, Stornetta RL & Guyenet PG. (2017). Blood Pressure Regulation by the Rostral Ventrolateral Medulla in Conscious Rats: Effects of Hypoxia, Hypercapnia, Baroreceptor Denervation, and Anesthesia. *J Neurosci* **37,** 4565-4583.

Wiley RG & Lappi DA. (1999). Targeting neurokinin-1 receptor-expressing neurons with [Sar9, Met(O2)11 substanceP-saporin. *Neurosci Lett* **27**

This article is protected by copyright. All rights reserved.

Accepted Article

Accepted Article

ADDITTIONAL INFORMATION

Competing interest

The authors declare they have no competing interest.

Author contributions

G.M.P.R.S., R.K, S.B.G.A., R.L.S. and P.G.G. designed the research; G.M.P.R.S., R.K. and D.S.S. performed the experiments; G.M.P.R.S., S.B.G.A and R.L.S. analyzed the data; G.M.P.R.S., R.L.S. and P.G.G. wrote the manuscript. All authors approved the final version of the manuscript and agree to be accountable for all aspects of the work in ensuring that questions related to the accuracy or integrity of any part of the work are appropriately investigated and resolved. All persons designated as authors qualify for authorship, and all those who qualify for authorship are listed.

Funding

This work was supported by grants from the National Institutes of Health (HL074011 and HL28785 to PGG).

Acknowledgements

None.

This article is protected by copyright. All rights reserved.

George Souza received a PhD in Physiology from the University of Sao Paulo, Brazil (2017). Currently, he is a post-doctoral fellow in the University of Virginia (UVA). He has been and still working on central control of breathing and blood pressure with focus on the role of specific brainstem neurons involved in these functions.

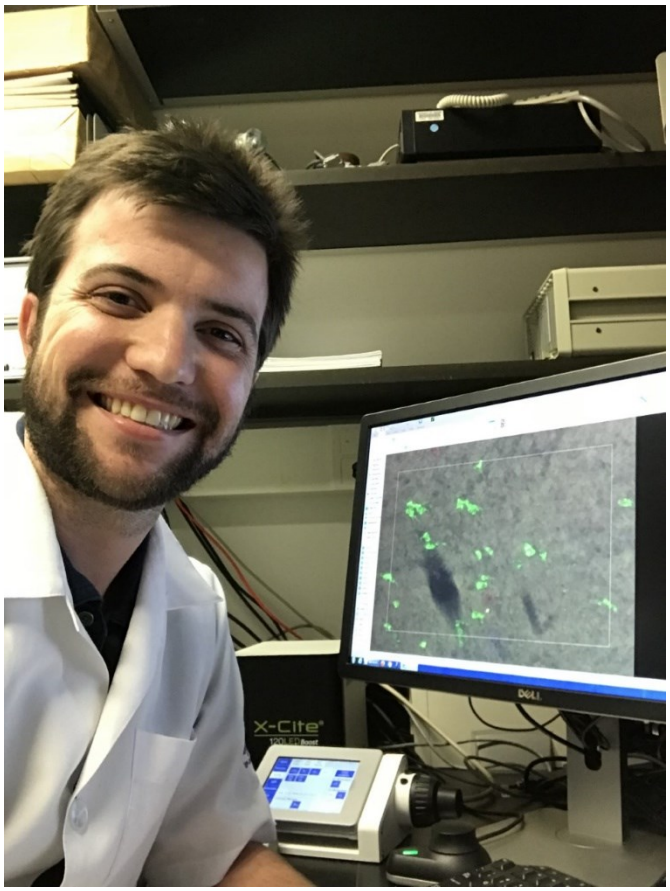

Accepted Article

This article is protected by copyright. All rights reserved.